In contrast, pools of negative control siRNA as well as CD13-specific siRNA did not significantly reduce JFH1 HCVcc infection (Fig. 4B). Taken together, reduced susceptibility to HCV infection by specific silencing of SR-BI expression clearly demonstrates that SR-BI plays a key role for the establishment of HCV infection of human hepatoma cells.

Impact of Lipoproteins for SR-BI–Mediated HCV Infection. To investigate the impact of lipoproteins on SR-BI–mediated HCV infection, we determined the ability of anti–SR-BI antibodies to inhibit JFH1 HCVcc infection in the absence of HDL, a physiological SR-BI ligand that has been shown to enhance HCVcc infection of human hepatoma cells.[35] To study the role of HDL during inhibition experiments, HCVcc were generated in medium supplemented with LPDS, and HDL was added extemporaneously for infection experiments. Fig. 5A shows that rat anti–SR-BI serum (rat 5) inhibited JFH1 HCVcc infection of Huh7.5 cells in the absence of HDL (Fig. 5A). Interestingly, whereas HDL was able to enhance JFH1 HCVcc infection in control cells and control serum preincubated cells, no such effect was observed in the presence of anti–SR-BI antibodies in concentrations blocking HCVcc infection (Fig. 5A). These results suggest that these antibodies may block both HCV interaction with SR-BI and HDL-mediated enhancing effect on HCVcc infection. To study whether HDL-dependent enhancement of HCVcc infection was dependent on the level of input virus, we repeated experiments using different JFH1 HCVcc preparations with challenge virus titers ranging from 1×10^7 copies/mL to 5×10^9 copies/mL, resulting in similar observations (data not shown). Furthermore, the effects of HDL on HCVcc infection were confirmed by titration experiments using anti–SR-BI antibodies: as shown in Fig. 5A, the enhancing effect of HDL on HCVcc infection appeared to be restored when anti–SR-BI antibodies were used at decreasing concentrations (Fig. 5A). In addition, the role of HDL on JFH1 HCVcc infection was also studied in siRNA-transfected Huh7.5 cells. As shown in Fig. 5B, a minor enhancing effect of HDL was detected in Huh7.5 cells transfected with siRNA targeting SR-BI, suggesting that a low level of SR-BI may still be available for HCV/HDL interplay on these cells. In cells with silenced CD81 expression, no marked enhancing effect of HDL on JFH1 HCVcc infection was observed (Fig. 5B).

SR-BI Mediates an HCV Entry Step Occurring Postbinding and Closely Linked to CD81. Kinetic studies using chimeric JFH1 firefly luciferase reporter virus have demonstrated that glycosaminoglycans predominantly act at the stage of HCV attachment to target cells, whereas CD81 mediates HCV infection at a step postbinding.[31] To map the step targeted by SR-BI during HCV entry, we investigated the inhibitory capacity of

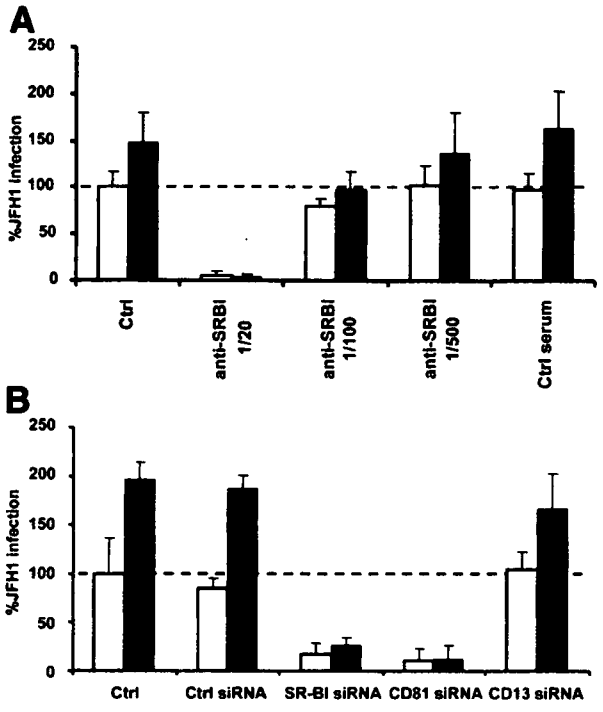

Fig. 5. SR-BI-mediated HCV infection is not dependent on the presence of lipoproteins. (A) Anti-SR-BI inhibits HCVcc infection in the absence of lipoproteins. Huh7.5 cells were preincubated for 1 hour at 37°C with rat anti-SR-BI serum or control serum (diluted 1/20, 1/100, and 1/500) before infection with JFH1 HCVcc generated in LPDS-medium in the presence (black bars) or absence (open bars) of HDL (30 μg/mL). Total RNA was isolated 72 hours after infection, and HCV RNA was quantified. Results are expressed as percent HCVcc infectivity in the absence of antibody (mean ± SD; n = 4). (B) Reduced susceptibility to HCVcc infection in SR-BI-specific siRNA expressing Huh7.5 cells is independent of lipoproteins. Control naïve Huh7.5 cells (Ctrl), Huh7.5 cells expressing control siRNA (Ctrl siRNA), or siRNA targeting SR-BI, CD81, or CD13 were incubated with JFH1 HCVcc generated in LPDS medium in the presence (black bars) or absence (open bars) of HDL (30 μg/mL). Total RNA was extracted 72 hours after infection, and HCV RNA was quantified. Data are expressed as mean percent HCVcc infectivity of naïve control cells (mean ± SD; n = 4).

anti–SR-BI serum (rat 5) and corresponding purified IgG when administered during or after virus binding in side-by-side experiments using heparin—a structural and functional homolog of highly sulfated heparan sulfate and anti-CD81 antibody. Luc-Jc1 HCVcc binding to Huh7.5 cells was performed for 1 hour at 4°C in the presence or absence of inhibitors. Under these conditions, virus attaches to the cells but does not efficiently enter, thus permitting synchronous infection when the inoculum is removed and cells are shifted to 37°C. Therefore, subsequent to virus attachment, unbound virus was washed away, cells were shifted to 37°C to allow entry to proceed, and inhibitors or control medium were added for 4 hours (Fig. 6A). Figure 6B shows that rat anti–SR-BI serum as well as purified anti–SR-BI IgG were able to inhibit Luc-Jc1 HCVcc infection when added following

binding of the virus to the target cell (Fig. 6B). The control serum only had no significant effect on Luc-Jc1 HCVcc infection (Fig. 6B). In contrast, heparin—a homolog of highly sulfated heparan sulfate, inhibited Luc-Jc1 HCVcc infection only when it was present during virus binding but not when added postbinding (Fig. 6B). To further characterize the entry step mediated by SR-BI, anti–SR-BI and anti-CD81 antibodies were added in side-by-side experiments every 20 minutes for up to 120 minutes after viral binding (Fig. 7A). Rat anti–SR-BI serum was able to inhibit Luc-Jc1 HCVcc infection even when added up to 60 minutes after HCVcc binding (Fig. 7B). These data clearly indicate that SR-BI is involved in an entry step occurring after binding. Because almost identical kinetics of inhibition of HCV infection was observed for anti-CD81 antibody assessed in side-by-side

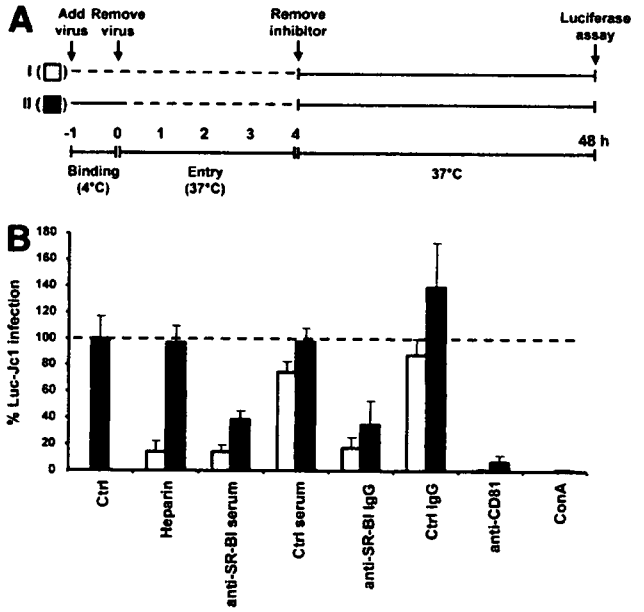

Fig. 6. SR-BI mediates in an HCV entry step occurring postbinding of virions. (A) Schematic drawing of the experimental setup. Inhibition of Luc-Jc1 HCVcc entry into Huh7.5 cells by rat anti-SR-BI serum or control serum (1/200), anti-SR-BI, or control IgG (100 μg/mL), anti-CD81 monoclonal antibody (10 μg/mL), heparin (250 μg/mL), or concanamycin A (25 nM) was compared using 2 different protocols. Virus binding to target cells was performed in the presence (protocol I) or absence (protocol II) of compounds. Subsequently, in both protocols, cells were washed, supplemented with fresh medium containing the given inhibitors, and shifted to 37°C to allow entry to proceed. Four hours later, cells were again washed and supplied with medium without inhibitors or antibodies. Dashed lines indicate the time intervals where inhibitors or antibodies were present. Luciferase activity was determined 48 hours later and is expressed relative to control infections performed in the same way but without addition of inhibitor. (B) Kinetics of HCVcc entry into human hepatoma cells. The efficiency of infection using the protocols depicted in panel A (protocol I: open bars; protocol II: black bars) was measured as described in (A). Results are expressed as percent Luc-Jc1 HCVcc infectivity in the absence of inhibitory compound or antibody (mean ± SD; n = 4).

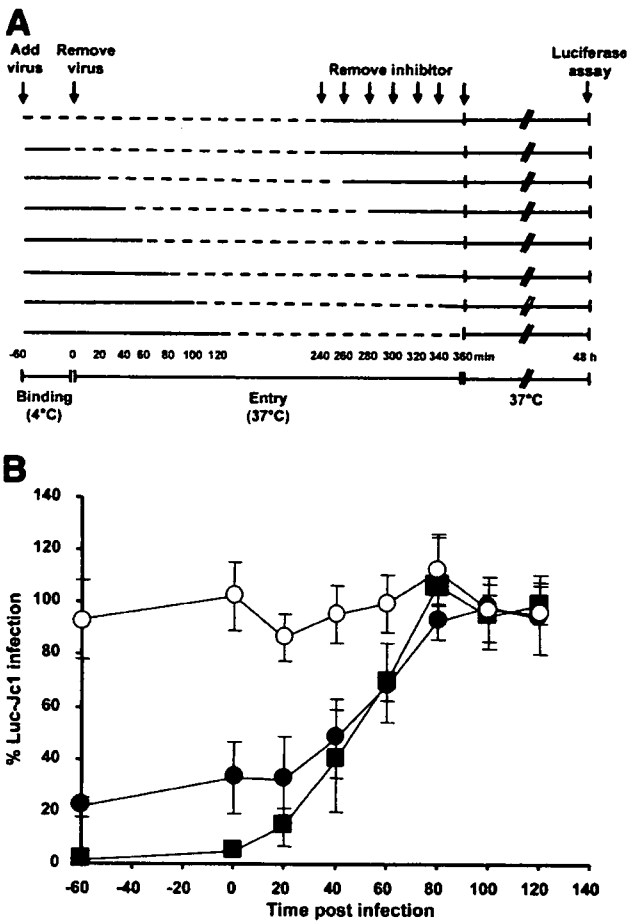

Fig. 7. SR-BI mediates an HCV entry step closely linked to CD81. (A) Schematic drawing of the experimental setup. Inhibition of Luc-Jc1 HCVcc entry into Huh7.5 cells by rat anti-SR-BI serum or control serum (1/200) as well as anti-CD81 monoclonal antibody (10 μg/mL) was performed as described in the legend to Fig. 6 but inhibitors were added every 20 minutes for 120 minutes after viral binding. Dashed lines indicate the time intervals where inhibitors are present. Luciferase activity was determined 48 hours later and is expressed relative to control infections performed in the same way but without addition of inhibitor. (B) Kinetics of HCVcc entry into human hepatoma cells. The efficiency of infection using rat anti-SR-BI serum (black circle), control serum (white circle), or anti-CD81 antibody (black square) was measured by luciferase assay 48 hours later. Results are expressed as percent Luc-Jc1 HCVcc infectivity in the absence of antibody (mean ± SD; n = 4).

experiments (Fig. 7B), it is likely that the entry steps mediated by SR-BI and CD81 occur during a similar time point and are closely linked to each other. To further address the contribution and interplay of CD81 and SR-BI in HCV entry, we added anti-CD81 and anti–SR-BI IgG simultaneously before Luc-Jc1 HCVcc infection. Figure 8B shows that blocking both CD81 and SR-BI inhibited Luc-Jc1 HCVcc infection more potently than blocking of each receptor alone (Fig. 8A,B). This effect was not observed when control IgG were used in combination with anti-CD81 monoclonal antibody (Fig.

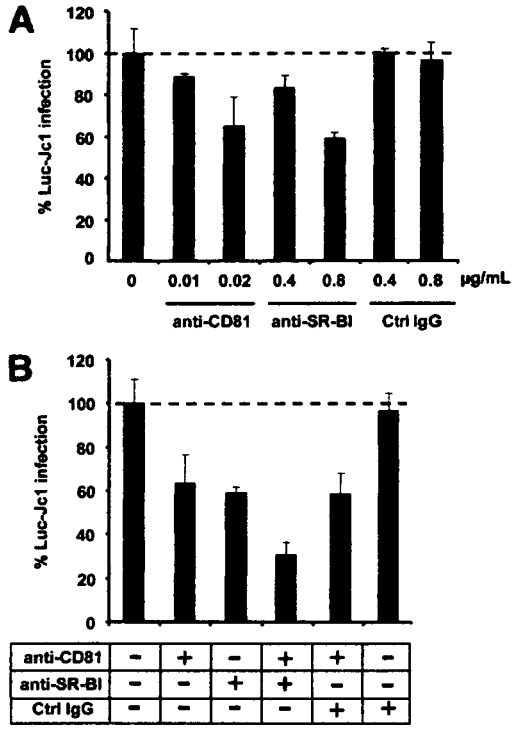

Fig. 8. SR-BI and CD81 act in concert to mediate HCV entry. (A) Dose-dependent inhibition of Luc-Jc1 HCVcc infectivity by anti-SR-BI and anti-CD81 antibodies. Huh7.5 cells were preincubated for 1 hour at 37°C with anti-CD81 monoclonal antibody (0.01 and 0.02 μg/mL), rat anti-SR-BI IgG (0.4 and 0.8 μg /mL) or control IgG (0.4 and 0.8 μg /mL) before infection with Luc-Jc1 HCVcc for 4 hours at 37°C. HCV infection was assessed by measurement of luciferase activity 48 hours after infection. Data are expressed as percent Luc-Jc1 HCVcc infectivity in the absence of antibody (mean ± SD; n = 4). (B) Additive effect of anti-SR-BI and anti-CD81 antibodies in inhibition of HCVcc entry. Huh7.5 cells were preincubated for 1 hour at 37°C with rat anti-SR-BI IgG (0.8 μg/mL) or control IgG (0.8 μg /mL) either alone or in combination with anti-CD81 monoclonal antibody (0.02 μg/mL) before infection with Luc-Jc1 HCVcc for 4 hours at 37°C. HCV infection was assessed as described in (A). Data are expressed as percent Luc-Jc1 HCVcc infectivity in the absence of antibody (mean ± SD; n = 4).

8B). Taken together, our results suggest that SR-BI and CD81 may act in concert to mediate HCV entry.

Discussion

Using an infectious HCV tissue culture system, we demonstrate that SR-BI (1) represents a key host factor for HCV entry, (2) is implicated in the same HCV entry pathway as CD81, and (3) targets an entry step occurring after binding closely linked to CD81.

SR-BI delivers HDL cholesteryl ester to the liver and steroidogenic tissues by a process termed the "selective uptake pathway."[36-39] This process differs markedly from that of the classic clathrin coated pit-mediated LDL receptor endocytic pathway, in which the entire lipoprotein is internalized and degraded.[40] In the selective uptake pathway, SR-BI binds HDL and the core cholesteryl ester are delivered to the plasma membrane without the endocytosis of the entire HDL particle. SR-BI–mediated selective HDL cholesteryl ester uptake is a 2-step process: the first step involves lipoprotein binding to the extracellular domain of SR-BI and the second step consists in the selective transfer of lipid to the plasma membrane.[41,42]

The marked inhibition of HCV infection of 2 different isolates (JFH1 and Jc1) by anti–SR-BI antibodies and siRNAs suggests that SR-BI plays a key role for establishment of HCV infection. These results extend recently obtained evidence suggesting that SR-Bs modulate HCV infection.[24,25] Extending previous studies, we demonstrate that inhibition of HCVcc infection by anti–SR-BI antibodies or SR-BI–specific siRNA was not dependent on the presence of lipoproteins in the tissue culture medium, suggesting that SR-BI can mediate HCV entry independent from an interaction of HCV or SR-BI with HDL. Lavillette et al.[17] demonstrated that silencing SR-BI expression markedly reduced HCVpp entry independent of HDL, whereas Voisset et al.[19] demonstrated that SR-BI silencing only reduced the HDL-mediated enhancement of HCVpp entry. Using the HCVcc model system and transfected siRNAs, we now demonstrate that silencing of SR-BI expression resulted in a marked down-regulation of susceptibility to HCV infection independent of the presence of lipoproteins, although HDL was able to enhance HCV infection. In our hands, the use of an optimal siRNA delivery system was crucial for the study of HCV infection. Whereas recombinant lentiviral vectors were characterized by interference with HCV infection unrelated to the expressed siRNA (data not shown), the transfection of *in vitro* transcribed SR-BI siRNAs specifically resulted in down-regulation of HCV infection The specific effect of SR-BI siRNAs is demonstrated by the lack of inhibitory effects of various control siRNAs including siRNAs targeting another protein expressed on the cell surface of hepatoma cells (CD13).

Because the presence of HDL did not inhibit but rather enhanced HCV infection, it is unlikely that HCV and HDL compete for the SR-BI HDL binding domain. The highly reproducible enhancement of HCV infection by HDL may point to a more efficient interaction of SR-BI with HCV, for example, as a result of a conformational change induced by HDL. These findings are in line with a previous study demonstrating that HDL is a serum factor that attenuates neutralization by antiviral antibodies of HCVpp or HCVcc.[33] The authors hypothesized that HDL may stimulate cell entry of viral particles by accelerating their endocytosis.[35] In contrast to results of ectodomain blocking by anti-SR-BI, HDL appeared to slightly enhance HCVcc infection in cells with silenced SR-BI. This may not be un-

expected because down-regulation by siRNA, in contrast to ectodomain blocking, most likely leaves some SR-BI accessible for HDL/HCV interplay.

Furthermore, we demonstrate that in target cells with silenced CD81 expression, HDL appeared not to markedly enhance HCVcc infection (Fig. 5B). These findings strongly suggest that the HDL/SR-BI-HCV interaction acts in concert with CD81 within the same entry pathway and does not represent another or redundant route of cell entry. This conclusion is further supported by an additive inhibitory effect of anti–SR-BI and anti-CD81 antibodies on Luc-Jc1 HCVcc infection (Fig. 8B), confirming previous results obtained for JFH1.[24]

Using an HCVcc-based kinetic entry assay (Figs. 6 and 7), we mapped the HCV entry step targeted by SR-BI. As shown in Figs. 6 and 7, anti–SR-BI IgG markedly inhibited HCVcc infection when added up to 60 minutes postbinding of attached virus. These data for the first time directly demonstrate that SR-BI predominantly mediates an HCV entry step occurring after binding of HCV to the hepatocyte cell surface membrane. These findings confirm the hypothesis raised by von Hahn and colleagues[20] based on experiments using oxidized lipoproteins as SR-BI ligands. In contrast to anti–SR-BI and anti-CD81 antibodies, heparin—a homolog of highly sulfated heparan sulfate—was able to inhibit HCVcc infection only when added before HCV binding. Taken together, these data suggest that glycosaminoglycans such as highly sulfated heparan sulfate act predominantly at the stage of viral attachment, whereas SR-BI and CD81 mediate entry steps occurring postbinding. Subsequent steps in HCV entry are most likely mediated by claudin-1, a recently discovered co-host factor for HCV infection.[6]

Kinetic studies using anti–SR-BI and CD81 antibodies in side-by-side experiments demonstrated that SR-BI is required for an entry step occurring at a similar time point as CD81–HCV interaction. Although the magnitude of antibody-mediated inhibition of HCVcc infection was different, the kinetics of inhibition of HCV infection by anti–SR-BI and anti-CD81 antibodies was remarkably similar (Fig. 6). Both anti–SR-BI and anti-CD81 antibodies were able to inhibit HCV infection when added up to 60 minutes after binding and lost their ability to inhibit HCV infection when added 80 minutes after binding. The rate of loss of CD81 antibody HCVcc inhibition overtime in our study appeared to be different from that observed for HCVpp in previously published studies.[6,43] This either may be due to experimental differences or may be a difference between the behaviors of HCVpp and HCVcc. Taken together, our results demonstrate that the entry steps mediated by SR-BI and CD81 occur during a similar time frame and are closely linked to each other.

SR-BI and its splicing variant SR-BII contain an identical extracellular domain. SR-BII is encoded by an alternatively spliced messenger RNA from the SR-BI gene and differs from SR-BI only in the carboxy-terminal cytoplasmic tail, which, as shown previously, must contain a signal that confers predominant intracellular expression and rapid endocytosis of HDL.[44] Scavenger receptor BII, which is expressed at low levels in the liver compared with SR-BI,[45] mediates rapid HDL endocytosis through a clathrin-dependent, caveolae-independent pathway,[44] but is inefficient compared with SR-BI in HDL cholesteryl ester selective uptake.[46] Because our tools (anti–SR-BI antibody and SR-BI siRNAs) also may target SR-BII, we cannot completely exclude a role for SR-BII in HCV infection as most recently shown by other investigators.[25]

In conclusion, our results demonstrate that SR-BI plays a key role for the establishment of HCV infection mediating HCV infection during an entry step occurring postbinding closely linked to the interaction of HCV with CD81. The functional mapping of SR-BI–HCV interaction and its impact for HCV entry has important implications for the understanding of the very first steps of HCV infection and the development of novel antiviral strategies targeting HCV entry.

Acknowledgment: We thank C. M. Rice (The Rockefeller University, New York, NY) for the gift of Huh7.5 cells and T. Huby (INSERM U551, Hôpital de la Pitié, Paris, France) for the gift of pcDNASR-BI/CLA-1. We are grateful to the Division of Clinical Chemistry, University Hospital Freiburg for providing HDL and LPDS. We also would like to acknowledge J. Dubuisson (Centre National de la Recherche Scientifique-UMR 8161, Institut de Biologie de Lille, Lille, France), J. McKeating (University of Birmingham, Birmingham, UK) and J.-L. Mandel (IGBMC, Strasbourg) for helpful discussions.

References

1. Chisari FV. Unscrambling hepatitis C virus-host interactions. Nature 2005;436:930-932.
2. Marsh M, Helenius A. Virus entry: open sesame. Cell 2006;124:729-740.
3. Pileri P, Uematsu Y, Campagnoli S, Galli G, Falugi F, Petracca R, et al. Binding of hepatitis C virus to CD81. Science 1998;282:938-941.
4. Bartosch B, Dubuisson J, Cosset FL. Infectious hepatitis C virus pseudoparticles containing functional E1–E2 envelope protein complexes. J Exp Med 2003;197:633-642.
5. Hsu M, Zhang J, Flint M, Logvinoff C, Cheng-Mayer C, Rice CM, et al. Hepatitis C virus glycoproteins mediate pH-dependent cell entry of pseudotyped retroviral particles. Proc Natl Acad Sci U S A 2003;100:7271-7276.
6. Evans MJ, von Hahn T, Tscherne DM, Syder AJ, Panis M, Wolk B, et al. Claudin-1 is a hepatitis C virus co-receptor required for a late step in entry. Nature 2007;446:801-805.
7. Barth H, Schäfer C, Adah MI, Zhang F, Linhardt RJ, Toyoda H, et al. Cellular binding of hepatitis C virus envelope glycoprotein E2 requires cell surface heparan sulfate. J Biol Chem 2003;278:41003-41012.

8. Agnello V, Abel G, Elfahal M, Knight GB, Zhang QX. Hepatitis C virus and other flaviviridae viruses enter cells via low density lipoprotein receptor. Proc Natl Acad Sci U S A 1999;96:12766-12771.
9. Scarselli E, Ansuini H, Cerino R, Roccasecca RM, Acali S, Filocamo G, et al. The human scavenger receptor class B type I is a novel candidate receptor for the hepatitis C virus. EMBO J 2002;21:5017-5025.
10. Krieger M. Scavenger receptor class B type I is a multiligand HDL receptor that influences diverse physiologic systems. J Clin Invest 2001;108:793-797.
11. Yamada E, Montoya M, Schuettler CG, Hickling TP, Tarr AW, Vitelli A, et al. Analysis of the binding of hepatitis C virus genotype 1a and 1b E2 glycoproteins to peripheral blood mononuclear cell subsets. J Gen Virol 2005;86:2507-2512.
12. Philips JA, Rubin EJ, Perrimon N. Drosophila RNAi screen reveals CD36 family member required for mycobacterial infection. Science 2005;309: 1251-1253.
13. Vishnyakova TG, Kurlander R, Bocharov AV, Baranova IN, Chen Z, Abu-Asab MS, et al. CLA-1 and its splicing variant CLA-2 mediate bacterial adhesion and cytosolic bacterial invasion in mammalian cells. Proc Natl Acad Sci U S A 2006;103:16888-16893.
14. Barth H, Cerino R, Arcuri M, Hoffmann M, Schurmann P, Adah MI, et al. Scavenger receptor class B type I and hepatitis C virus infection of primary tupaia hepatocytes. J Virol 2005;79:5774-5785.
15. Lavillette D, Morice Y, Germanidis G, Donot P, Soulier A, Pagkalos E, et al. Human serum facilitates hepatitis C virus infection, and neutralizing responses inversely correlate with viral replication kinetics at the acute phase of hepatitis C virus infection. J Virol 2005;79:6023-6034.
16. Bartosch B, Vitelli A, Granier C, Goujon C, Dubuisson J, Pascale S, et al. Cell entry of hepatitis C virus requires a set of co-receptors that include the CD81 tetraspanin and the SR-B1 scavenger receptor. J Biol Chem 2003; 278:41624-41630.
17. Lavillette D, Tarr AW, Voisset C, Donot P, Bartosch B, Bain C, et al. Characterization of host-range and cell entry properties of the major genotypes and subtypes of hepatitis C virus. HEPATOLOGY 2005;41:265-274.
18. Bartosch B, Verney G, Dreux M, Donot P, Morice Y, Penin F, et al. An interplay between hypervariable region 1 of the hepatitis C virus E2 glycoprotein, the scavenger receptor BI, and high-density lipoprotein promotes both enhancement of infection and protection against neutralizing antibodies. J Virol 2005;79:8217-8229.
19. Voisset C, Callens N, Blanchard E, Op De Beeck A, Dubuisson J, Vu-Dac N. High density lipoproteins facilitate hepatitis C virus entry through the scavenger receptor class B type I. J Biol Chem 2005;280:7793-7799.
20. von Hahn T, Lindenbach BD, Boullier A, Quehenberger O, Paulson M, Rice CM, et al. Oxidized low-density lipoprotein inhibits hepatitis C virus cell entry in human hepatoma cells. HEPATOLOGY 2006;43:932-942.
21. Wakita T, Pietschmann T, Kato T, Date T, Miyamoto M, Zhao Z, et al. Production of infectious hepatitis C virus in tissue culture from a cloned viral genome. Nat Med 2005;11:791-796.
22. Lindenbach BD, Evans MJ, Syder AJ, Wolk B, Tellinghuisen TL, Liu CC, et al. Complete replication of hepatitis C virus in cell culture. Science 2005;309:623-626.
23. Zhong J, Gastaminza P, Cheng G, Kapadia S, Kato T, Burton DR, et al. Robust hepatitis C virus infection in vitro. Proc Natl Acad Sci U S A 2005;102:9294-9299.
24. Kapadia SB, Barth H, Baumert T, McKeating JA, Chisari FV. Initiation of hepatitis C virus Infection is dependent on cholesterol and cooperativity between CD81 and scavenger receptor B type I. J Virol 2007;81:374-383.
25. Grove J, Huby T, Stamataki Z, Vanwolleghem T, Meuleman P, Farquhar M, et al. Scavenger receptor BI and BII expression levels modulate hepatitis C virus infectivity. J Virol 2007;81:3162-3169.
26. Wellnitz S, Klumpp B, Barth H, Ito S, Depla E, Dubuisson J, et al. Binding of hepatitis C virus-like particles derived from infectious clone H77C to defined human cell lines. J Virol 2002;76:1181-1193.
27. Blight KJ, McKeating JA, Rice CM. Highly permissive cell lines for subgenomic and genomic hepatitis C virus RNA replication. J Virol 2002;76: 13001-13014.
28. Codran A, Royer C, Jaeck D, Bastien-Valle M, Baumert TF, Kieny MP, et al. Entry of hepatitis C virus pseudotypes into primary human hepatocytes by clathrin-dependent endocytosis. J Gen Virol 2006;87:2583-2593.
29. Schoonjans K, Annicotte JS, Huby T, Botrugno OA, Fayard E, Ueda Y, et al. Liver receptor homolog 1 controls the expression of the scavenger receptor class B type I. EMBO Rep 2002;3:1181-1187.
30. Pietschmann T, Kaul A, Koutsoudakis G, Shavinskaya A, Kallis S, Steinmann E, et al. Construction and characterization of infectious intragenotypic and intergenotypic hepatitis C virus chimeras. Proc Natl Acad Sci U S A 2006;103:7408-7413.
31. Koutsoudakis G, Kaul A, Steinmann E, Kallis S, Lohmann V, Pietschmann T, et al. Characterization of the early steps of hepatitis C virus infection by using luciferase reporter viruses. J Virol 2006;80:5308-5320.
32. Kato T, Date T, Miyamoto M, Furusaka A, Tokushige K, Mizokami M, et al. Efficient replication of the genotype 2a hepatitis C virus subgenomic replicon. Gastroenterology 2003;125:1808-1817.
33. Nauck M, Winkler K, Marz W, Wieland H. Quantitative determination of high-, low-, and very-low-density lipoproteins and lipoprotein(a) by agarose gel electrophoresis and enzymatic cholesterol staining. Clin Chem 1995;41:1761-1767.
34. Takeuchi T, Katsume A, Tanaka T, Abe A, Inoue K, Tsukiyama-Kohara K, et al. Real-time detection system for quantification of hepatitis C virus genome. Gastroenterology 1999;116:636-642.
35. Dreux M, Pietschmann T, Granier C, Voisset C, Ricard-Blum S, Mangeot PE, et al. High density lipoprotein inhibits hepatitis C virus-neutralizing antibodies by stimulating cell entry via activation of the scavenger receptor BI. J Biol Chem 2006;281:18285-18295.
36. Acton S, Rigotti A, Landschulz KT, Xu S, Hobbs HH, Krieger M. Identification of scavenger receptor SR-BI as a high density lipoprotein receptor. Science 1996;271:518-520.
37. Glass C, Pittman RC, Civen M, Steinberg D. Uptake of high-density lipoprotein-associated apoprotein A-I and cholesterol esters by 16 tissues of the rat in vivo and by adrenal cells and hepatocytes in vitro. J Biol Chem 1985;260:744-750.
38. Glass C, Pittman RC, Weinstein DB, Steinberg D. Dissociation of tissue uptake of cholesterol ester from that of apoprotein A-I of rat plasma high density lipoprotein: selective delivery of cholesterol ester to liver, adrenal, and gonad. Proc Natl Acad Sci U S A 1983;80:5435-5439.
39. Reaven E, Chen YD, Spicher M, Azhar S. Morphological evidence that high density lipoproteins are not internalized by steroid-producing cells during in situ organ perfusion. J Clin Invest 1984;74:1384-1397.
40. Brown MS, Goldstein JL. A receptor-mediated pathway for cholesterol homeostasis. Science 1986;232:34-47.
41. Gu X, Trigatti B, Xu S, Acton S, Babitt J, Krieger M. The efficient cellular uptake of high density lipoprotein lipids via scavenger receptor class B type I requires not only receptor-mediated surface binding but also receptor-specific lipid transfer mediated by its extracellular domain. J Biol Chem 1998;273:26338-26348.
42. Connelly MA, Klein SM, Azhar S, Abumrad NA, Williams DL. Comparison of class B scavenger receptors, CD36 and scavenger receptor BI (SR-BI), shows that both receptors mediate high density lipoprotein-cholesteryl ester selective uptake but SR-BI exhibits a unique enhancement of cholesteryl ester uptake. J Biol Chem 1999;274:41-47.
43. Bertaux C, Dragic T. Different domains of CD81 mediate distinct stages of hepatitis C virus pseudoparticle entry. J Virol 2006;80:4940-4948.
44. Eckhardt ER, Cai L, Shetty S, Zhao Z, Szanto A, Webb NR, et al. High density lipoprotein endocytosis by scavenger receptor SR-BII is clathrin-dependent and requires a carboxyl-terminal dileucine motif. J Biol Chem 2006;281:4348-4353.
45. Webb NR, de Villiers WJ, Connell PM, de Beer FC, van der Westhuyzen DR. Alternative forms of the scavenger receptor BI (SR-BI). J Lipid Res 1997;38:1490-1495.
46. Eckhardt ER, Cai L, Sun B, Webb NR, van der Westhuyzen DR. High density lipoprotein uptake by scavenger receptor SR-BII. J Biol Chem 2004;279:14372-14381.

JOURNAL OF VIROLOGY, Dec. 2007, p. 13922–13926
0022-538X/07/$08.00+0 doi:10.1128/JVI.01517-07

Vol. 81, No. 24

DDX3 DEAD-Box RNA Helicase Is Required for Hepatitis C Virus RNA Replication▽

Yasuo Ariumi,[1] Misao Kuroki,[1] Ken-ichi Abe,[1] Hiromichi Dansako,[1] Masanori Ikeda,[1] Takaji Wakita,[2] and Nobuyuki Kato[1]*

Department of Molecular Biology, Okayama University Graduate School of Medicine, Dentistry, and Pharmaceutical Sciences, 2-5-1, Shikata-cho, Okayama 700-8558,[1] and Department of Virology II, National Institute of Infectious Diseases, Toyama 1-23-1, Shinjuku-ku, Tokyo 162-8640,[2] Japan

Received 11 July 2007/Accepted 5 September 2007

DDX3, a DEAD-box RNA helicase, binds to the hepatitis C virus (HCV) core protein. However, the role(s) of DDX3 in HCV replication is still not understood. Here we demonstrate that the accumulation of both genome-length HCV RNA (HCV-O, genotype 1b) and its replicon RNA were significantly suppressed in HuH-7-derived cells expressing short hairpin RNA targeted to DDX3 by lentivirus vector transduction. As well, RNA replication of JFH1 (genotype 2a) and release of the core into the culture supernatants were suppressed in DDX3 knockdown cells after inoculation of the cell culture-generated HCVcc. Thus, DDX3 is required for HCV RNA replication.

DEAD-box RNA helicases are involved in various RNA metabolic processes, including transcription, translation, RNA splicing, RNA transport, and RNA degradation (9, 20). DDX1 and DDX3, DEAD-box RNA helicases, have been implicated in the replication of human immunodeficiency virus type 1 (HIV-1). Both DDX1 and DDX3 interact with HIV-1 Rev and enhance Rev-dependent HIV-1 RNA nuclear export (10, 24).

On the other hand, DDX3 binds to the hepatitis C virus (HCV) core protein (17, 19, 25), and DDX3 expression is deregulated in HCV-associated hepatocellular carcinoma (HCC) (7, 8). However, the biological function of DDX3 in HCV replication is still not understood. To address this issue, we first used lentivirus vector-mediated RNA interference to stably knock down DDX3 in three HuH-7-derived cell lines: O cells, harboring a replicative genome-length HCV RNA (HCV-O, genotype 1b) (13); sO cells, harboring its subgenomic replicon of HCV RNA (14); or RSc cured cells, which cell culture-generated HCV (HCVcc) (JFH1, genotype 2a) (23) could infect and effectively replicate in (M. Ikeda et al., unpublished data). Oligonucleotides with the following sense and antisense sequences were used for the cloning of short hairpin RNA (shRNA)-encoding sequences against DDX3 in the lentivirus vector: for DDX3i#3, 5′-GATCCCCGGAGGA AATTATAACTCCCTTCAAGAGAGGGAGTTATAATTT CCTCCTTTTTGGAAA-3′ (sense) and 5′-AGCTTTTCCAA AAAGGAGGAAATTATAACTCCCTCTCTTGAAGGGA GTTATAATTTCCTCCGGG-3′ (antisense); for DDX3i#7, 5′-GATCCCCGGTCACCCTGCCAAACAAGTTCAAGAG ACTTGTTTGGCAGGGTGACCTTTTTGGAAA-3′ (sense) and 5′-AGCTTTTCCAAAAAGGTCACCCTGCCAAACAA GTCTCTTGAACTTGTTTGGCAGGGTGACCGGG-3′ (antisense). These oligonucleotides were annealed and subcloned into the BglII-HindIII site, downstream from an RNA polymerase III promoter of pSUPER (6). To construct pLV-DDX3i#3 and pLV-DDX3i#7, the BamHI-SalI fragments of the corresponding pSUPER plasmids were subcloned into the BamHI-SalI site of pRDI292 (5), an HIV-1-derived self-inactivating lentivirus vector containing a puromycin resistance marker allowing for the selection of transduced cells. The vesicular stomatitis virus G protein (VSV-G)-pseudotyped HIV-1-based vector system has been described previously (18). We used the second-generation packaging construct pCMV-ΔR8.91 (26) and the VSV-G-envelope plasmid pMDG2. The lentivirus vector particles were produced by transient transfection of 293FT cells with FuGene 6 (Roche).

Western blot analysis of the lysates demonstrated the only trace of DDX3 protein in DDX3 knockdown O cells (DDX3i#3) (Fig. 1A). In this context, the HCV core expression level was significantly decreased in the DDX3 knockdown O cells (Fig. 1A). To further confirm this finding, we examined the level of HCV RNA in these cells. We found that accumulation of genome-length HCV-O RNA was notably suppressed in DDX3 knockdown O cells (Fig. 1B). Furthermore, the efficiency of colony formation in DDX3 knockdown Oc cells (created by eliminating genome-length HCV RNA from O cells by interferon treatment) transfected with the genome-length HCV-O RNA with an adapted mutation at amino acid (aa) position 1609 in the NS3 helicase region (K1609E) (13) was also notably reduced compared with that in control cells (Fig. 1C). In contrast, highly efficient knockdown of an unrelated host factor, poly(ADP-ribose) polymerase 1 (PARP-1) (4), had no observable effects on HCV RNA replication, the efficiency of colony formation, or the core expression level (data not shown), suggesting that our finding was not due to a nonspecific event. Interestingly, accumulation of the subgenomic replicon RNA (HCV-sO) was also suppressed in DDX3 knockdown sO cells (Fig. 1D). Moreover, we examined the potential role of DDX3 in an HCV infection and produc-

* Corresponding author. Mailing address: Department of Molecular Biology, Okayama University Graduate School of Medicine, Dentistry, and Pharmaceutical Sciences, 2-5-1, Shikata-cho, Okayama 700-8558, Japan. Phone: 81 86 235 7386. Fax: 81 86 235 7392. E-mail: nkato@md.okayama-u.ac.jp.

▽ Published ahead of print on 12 September 2007.

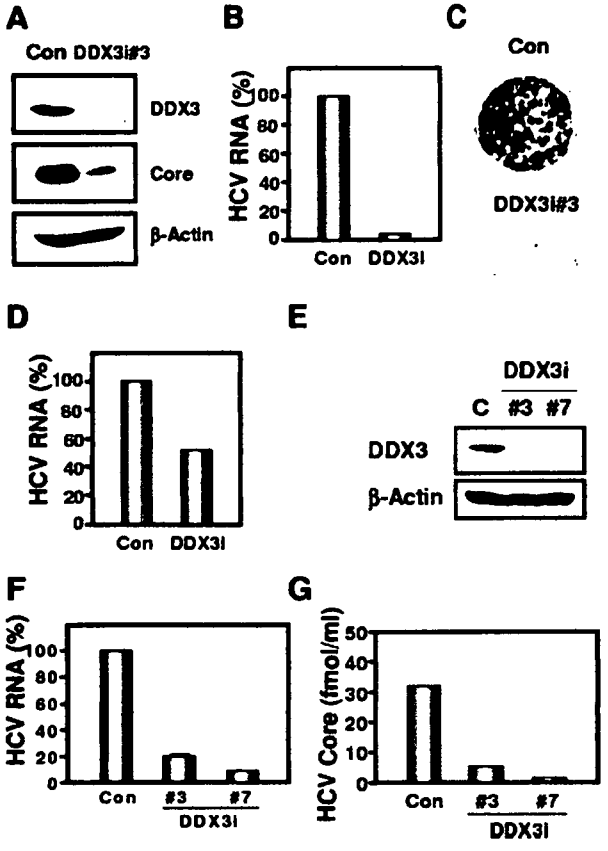

FIG. 1. Requirement of DDX3 for HCV replication. (A to D) Effect of DDX3 knockdown on HCV RNA replication. (A) Inhibition of DDX3 expression by shRNA-producing lentivirus vector. The results of Western blot analysis of cellular lysates with anti-DDX3 (ProSci), anti-HCV core (CP-9; Institute of Immunology), or an anti-β-actin antibody (Sigma) in O cells expressing shRNA against DDX3 (DDX3i#3) as well as in O cells transduced with a control lentivirus vector (Con) are shown. (B) The level of genome-length HCV RNA was monitored by real-time LightCycler PCR (Roche). Experiments were done in duplicate, and bars represent the mean percentages of HCV RNA. (C) Efficiency of colony formation in DDX3 knockdown cells. In vitro-transcribed ON/C-5B K1609E RNA (2 μg) was transfected into the DDX3 knockdown Oc cells (DDX3i#3) or the Oc cells transduced with a control lentivirus vector (Con). G418-resistant colonies were stained with Coomassie brilliant blue at 3 weeks after electroporation of RNA. Experiments were done in duplicate, and representative results are shown. (D) The level of subgenomic replicon RNA was monitored by real-time LightCycler PCR. Experiments were done in duplicate, and bars represent the mean percentages of HCV RNA. (E to G) Effect of DDX3 knockdown on HCV infection. (E) Inhibition of DDX3 expression by shRNA-producing lentivirus vector. The results of Western blot analysis of cellular lysates with anti-DDX3 or an anti-β-actin antibody for RSc cells expressing the shRNA DDX3i#3 or DDX3i#7 and for RSc cells transduced with a control lentivirus vector (Con) are shown. (F) The level of genome-length HCV (JFH1) RNA was monitored by real-time LightCycler PCR after inoculation of the cell culture-generated HCVcc. Results from three independent experiments are shown. (G) The levels of the HCV core in the culture supernatants were determined by an enzyme-linked immunosorbent assay (Mitsubishi Kagaku Bio-Clinical Laboratories). Experiments were done in duplicate, and bars represent the mean HCV core protein levels.

tion system (23). We found 80 to 90% reductions in the accumulation of JFH1 RNA and 82 to 94% reductions in the release of the core into the culture supernatants in DDX3 knockdown HuH-7-derived RSc cured cells at 4 days after inoculation of HCVcc (Fig. 1E to G). Thus, DDX3 seems to be required for HCV RNA replication.

Previously, DDX3 was identified as an HCV core-interacting protein by yeast two-hybrid screening. This interaction required the N-terminal domain of the core (aa 1 to 59) and the C-terminal domain of DDX3 (aa 553 to 622) (17, 19, 25). To determine whether the core can interact with DDX3 regardless of the HCV genotype, we used the HCV-O core (genotype 1b) and the JFH1 core (genotype 2a) (Table 1). We first examined their subcellular localization by confocal laser scanning microscopy as previously described (3). Consistent with previous reports (17, 19, 25), both the HCV-O core and JFH1 core mostly colocalized with DDX3 in the perinuclear region (Fig. 2A). Then we immunoprecipitated lysates from 293FT cells in which hemagglutinin (HA)-tagged DDX3 and HCV-O core, JFH1 core, or their 40-aa N-truncated mutants were overexpressed with an anti-HA antibody. Cells were lysed in a buffer containing 50 mM Tris-HCl (pH 8.0), 150 mM NaCl, 4 mM EDTA, 0.5% NP-40, 10 mM NaF, 0.1 mM Na_3VO_4, 1 mM dithiothreitol, and 1 mM phenylmethylsulfonyl fluoride. Lysates were precleared with 30 μl of protein G-Sepharose (GE Healthcare Bio-Sciences). Precleared supernatants were incubated with 1 μg of anti-HA antibody (3F10; Roche) at 4°C for 1 h. Following absorption of the precipitates

TABLE 1. Primers used for construction of the HCV core-expressing plasmids[a]

Plasmid name	Direction	Primer sequence
pCXbsr/core(HCV-O)	Forward	5'-GGAATTCCCACCATGAG CACGAATCCTAAACCTC-3
	Reverse	5'-ATAAGAATGCGGCCGCC TATCAAGCGGAAGCTGG GATGGT-3'
pcDNA3/core(HCV-O)	Forward	5'-CGGGATCCAAGATGAGC ACGAATCCTAAACCTCAA AGA-3'
pcDNA3/FLAG-core(HCV-O)	Reverse	5'-CCGCTCGAGTCAAGCGG AAGCTGGGATGGTCAAA CA-3'
pcDNA3/Δcore(HCV-O)	Forward	5'-CGGGATCCAAGATGGGC CCCAGGTTGGGTGTGCG C-3'
pcDNA3/FLAG-Δcore(HCV-O)	Reverse	5'-CCGCTCGAGTCAAGCGG AAGCTGGGATGGTCAAA CA-3'
pcDNA3/core(JFH1)	Forward	5'-CGGGATCCAAGATGAGC ACAAATCCTAAACCTCAA AGA-3'
pcDNA3/FLAG-core(JFH1)	Reverse	5'-CCGCTCGAGTCAAGCAG AGACCGGAACGGTGATG CA-3'
pcDNA3/Δcore(JFH1)	Forward	5'-CGGGATCCAAGATGGGC CCCAGGTTGGGTGTGCG C-3'
pcDNA3/FLAG-Δcore(JFH1)	Reverse	5'-CCGCTCGAGTCAAGCAG AGACCGGAACGGTGATG CA-3'

[a] To construct pCXbsr/core(HCV-O), a DNA fragment encoding the core was amplified by PCR from pON/C-5B (13) with the indicated primers. The PCR product was digested with EcoRI-NotI and subcloned into the same site of pCX4bsr (1). To construct pcDNA3/core(HCV-O), pcDNA3/FLAG-core(HCV-O), pcDNA3/Δcore(HCV-O), and pcDNA3/FLAG-Δcore(HCV-O), DNA fragments encoding the core were amplified by PCR from pON/C-5B (13) with the indicated primer sets. To construct pcDNA3/core(JFH1), pcDNA3/FLAG-core(JFH1), pcDNA3/Δcore(JFH1), and pcDNA3/FLAG-Δcore(JFH1), DNA fragments encoding the core were amplified by PCR from pJFH1 (23) with the indicated primer sets. The PCR products were digested with BamHI and XhoI and then subcloned into the same site of pcDNA3 (Invitrogen) or pcDNA3-FLAG (2).

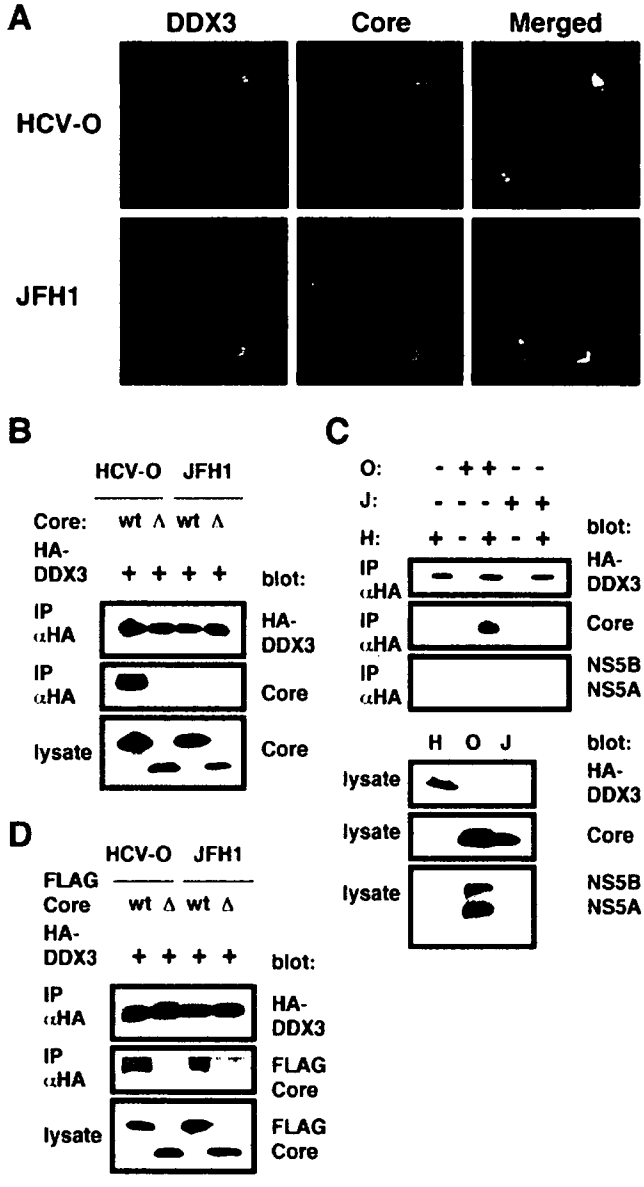

FIG. 2. Interaction of the HCV core with DDX3. (A) The HCV core colocalizes with DDX3. 293FT cells cotransfected with 100 ng of pCXbsr/core(HCV-O) or pcDNA3/core(JFH1) and 200 ng of pHA-DDX3 were examined by confocal laser scanning microscopy. Cells were stained with anti-HCV core (CP-9 and CP-11 mixture) and anti-DDX3 antibodies and were then visualized with fluorescein isothiocyanate (DDX3) or Cy3 (core). Images were visualized using confocal laser scanning microscopy (LSM510; Carl Zeiss). The right panels exhibit the two-color overlay images (Merged). Colocalization is shown in yellow. (B) The core binds to DDX3. 293FT cells were cotransfected with 4 μg of pHA-DDX3 and 4 μg of pCXbsr/core(HCV-O) (wt), pcDNA3/Δcore(HCV-O) (Δ), pcDNA3/core(JFH1) (wt), or pcDNA3/Δcore(JFH1) (Δ). The cell lysates were immunoprecipitated with an anti-HA antibody (3F10; Roche), followed by immunoblot analysis using either anti-HA (HA-7; Sigma) or anti-HCV core antibody (CP-9 and CP-11 mixture). (C) 293FT cells transfected with 4 μg of pHA-DDX3 (H), O cells (O), or RSc cells 3 days after inoculation of HCVcc (JFH1) (J) were lysed and immunoprecipitated (IP) with 1 μg of anti-HA antibody (3F10), followed by immunoblotting with anti-HA (HA-7), anti-core (CP-9 and CP-11 mixture), or anti-HCV NS5A (no. 8926) and anti-HCV NS5B. (D) 293FT cells transfected with 4 μg of pHA-DDX3 and 4 μg of pcDNA3/FLAG-core(HCV-O) (wt), pcDNA3/FLAG-Δcore(HCV-O) (Δ), pcDNA3/FLAG-core(JFH1) (wt), or pcDNA3/FLAG-Δcore(JFH1) (Δ) were lysed and immunoprecipitated with 1 μg of an anti-HA antibody (3F10), followed by immunoblotting with an anti-HA (HA-7) or anti-core (CP-9 and CP-11 mixture) antibody.

on 30 μl of protein G-Sepharose resin for 1 h, the resin was washed four times with 700 μl lysis buffer. Proteins were eluted by boiling the resin for 5 min in 1× Laemmli sample buffer. The proteins were then subjected to sodium dodecyl sulfate-polyacrylamide gel electrophoresis, followed by immunoblot analysis using either anti-HA (HA-7; Sigma) or anti-HCV core antibody (CP-9 and CP-11 mixture). We observed that the HCV-O core but not its N-truncated mutant could strongly bind to HA-tagged DDX3 (Fig. 2B). In contrast, the binding activity of the JFH1 core to HA-tagged DDX3 seemed to be fairly weak (Fig. 2B). As well, immunoprecipitation of lysates of 293FT cells expressing HA-tagged DDX3, O cells, or JFH1-infected RSc cells, or mixtures of these lysates, with an anti-HA antibody revealed that HCV-O core but not JFH1 core could bind strongly to DDX3 (Fig. 2C). The anti-HCV core antibody we used could detect both HCV-O core and JFH1 core (Fig. 2), while both anti-HCV NS5A and anti-NS5B antibodies failed to detect JFH1 NS5A and NS5B (Fig. 2C). At least, we failed to detect an interaction between DDX3 and either HCV-O NS5A or NS5B under experimental conditions that permitted the core to interact with DDX3 by immunoprecipitation (Fig. 2C). In contrast, the FLAG-tagged JFH1 core could bind to HA-tagged DDX3 just as efficiently as the FLAG-tagged HCV-O core could (Fig. 2D). Thus, the binding affinity or stability of the complex formed between the JFH1 core and DDX3 might be weaker than that between the HCV-O core and DDX3.

Since DDX3 is required for HIV-1 and HCV replication, we hypothesized that the HCV core might affect the function of HIV-1 Rev when both proteins were coexpressed. To test this hypothesis, we used the Rev-dependent luciferase-based reporter plasmid pDM628, harboring a single intron that includes both the Rev-responsive element (RRE) and the luciferase coding sequences (Fig. 3A) (10). In this system, Rev binds to RRE on the unspliced reporter mRNA, allowing its export from the nucleus for luciferase reporter gene expression, while the intron containing the luciferase gene is excised during RNA splicing when cells are transiently transfected with pDM628 alone. As previously reported (10), the luciferase activity in 293FT cells transfected with this reporter plasmid was stimulated by Rev, which induced a fourfold increase in the reporter signal (Fig. 3B). Luciferase activity was increased eightfold by the combination of Rev and DDX3, whereas neither the HCV-O core nor the JFH1 core had any effect on this Rev function (Fig. 3B). Since the Rev-binding domain (the N-terminal domain) and the core-binding domain (the C-terminal domain) do not overlap in DDX3, the HCV core might not compete with HIV-1 Rev for binding with DDX3. However, the development of a novel DDX3 inhibitor might provide a powerful antiviral agent against both HIV-1 and HCV (15).

Taking these results together, this study has shown for the first time that DDX3 is required for HCV RNA replication.

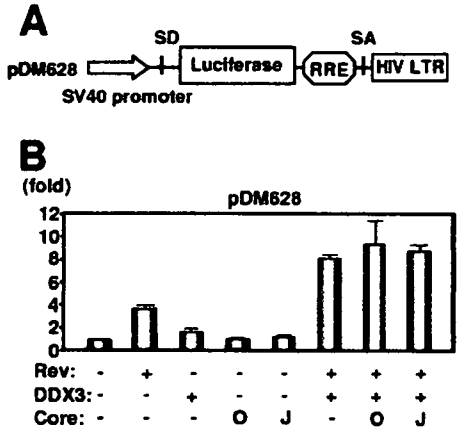

FIG. 3. HCV core does not affect the DDX3-mediated synergistic activation of Rev function. (A) Schematic representation of HIV-1 Rev-dependent luciferase-based reporter plasmid pDM628 harboring a splicing donor (SD), splicing acceptor (SA), and RRE. (B) 293FT cells were cotransfected with 100 ng of pDM628, 200 ng of pcRev, 200 ng of pHA-DDX3, and/or 100 ng of either pcDNA3/core(HCV-O) (O) or pcDNA3/core(JFH1) (J). A luciferase assay was performed 24 h later. All transfections utilized equal total amounts of plasmid DNA owing to the addition of the empty vector pcDNA3 to the transfection mixture. The relative stimulation of luciferase activity (*n*-fold) is shown. The results shown are means from three independent experiments.

Since helicases are motor enzymes that use energy derived from nucleoside triphosphate hydrolysis to unwind double-stranded nucleic acids, the DDX3–core complex might unwind the HCV double-stranded RNA and separate the RNA strands or might contribute to the function of HCV NS3 helicase. Since the replication of subgenomic replicon RNA was also partially suppressed in DDX3 knockdown cells (Fig. 1D), DDX3 might be associated with an HCV nonstructural protein(s) or HCV RNA itself. Indeed, Tingting et al. recently reported that DDX1 bound to both the HCV 3′ untranslated region (3′ UTR) and the HCV 5′ UTR and that short interfering RNA-mediated knockdown of DDX1 caused a marked reduction in the replication of subgenomic replicon RNA (22). Furthermore, Goh et al. demonstrated that DDX5/p68 associated with HCV NS5B and that depletion of endogenous DDX5 correlated with a reduction in the transcription of negative-strand HCV RNA (11). However, we failed to observe an interaction between DDX3 and NS5A or NS5B by immunoprecipitation under our experimental conditions in which the core could interact with DDX3 (Fig. 2C). Importantly, our DDX3 knockdown study demonstrated a more significant reduction in the accumulation of genome-length HCV RNA (95% reduction) than in the accumulation of subgenomic replicon RNA (52% reduction) (Fig. 1B and D). To date, it has been demonstrated that the 5′ UTR, the 3′ UTR, and the NS3-to-NS5B coding region are sufficient for HCV RNA replication (16); however, the core might be partly involved in the replication of genome-length HCV RNA. Importantly, DDX1 and DDX3 were specifically detected in the lipid droplets of core-expressing Hep39 cells by proteomic analysis (21), suggesting that DDX3 might be associated with HCV assembly or might incorporate into the HCV virion through interaction with the core to act as an RNA chaperone.

Recent studies have suggested a potential role of DDX3 and DDX5 in the pathogenesis of HCV-related liver diseases. DDX3 expression is deregulated in HCV-associated HCC (7, 8), and Huang et al. identified single-nucleotide polymorphisms in the DDX5 gene that were significantly associated with an increased risk of advanced fibrosis in patients with chronic hepatitis C (12). Interestingly, DDX3 might be a candidate tumor suppressor. DDX3 inhibits colony formation in various cell lines, including HuH-7, and up-regulates the $p21^{waf1/cip1}$ promoter (8). If DDX3 could in fact suppress tumor growth, then the core might overcome DDX3-mediated cell growth arrest and down-regulate $p21^{waf1/cip1}$ through interaction with DDX3, and it might also be involved in HCC development.

We thank D. Trono, K.-T. Jeang, V. Yedavalli, R. J. Pomerantz, J. Fang, R. Iggo, M. Hijikata, T. Akagi, and M. Kohara for pCMVΔR8.91, pMDG2, pHA-DDX3, pDM628, pcRev, pSUPER, pRDI292, 293FT cells, pCX4bsr, and the anti-NS5B antibody. We also thank A. Morishita and T. Nakamura for technical assistance.

This work was supported by a Grant-in-Aid for Young Scientists (B) from the Ministry of Education, Culture, Sports, Science, and Technology (MEXT), by a Grant-in-Aid for Research on Hepatitis from the Ministry of Health, Labor, and Welfare of Japan, by the Naito Foundation, by the Ichiro Kanehara foundation, and by a research fellowship from the Japan Society for the Promotion of Science (JSPS).

REFERENCES

1. **Akagi, T., T. Shishido, K. Murata, and H. Hanafusa.** 2000. v-Crk activates the phosphoinositide 3-kinase/AKT pathway in transformation. Proc. Natl. Acad. Sci. USA **97**:7290–7295.
2. **Ariumi, Y., A. Kaida, M. Hatanaka, and K. Shimotohno.** 2001. Functional cross-talk of HIV-1 Tat with p53 through its C-terminal domain. Biochem. Biophys. Res. Commun. **287**:556–561.
3. **Ariumi, Y., T. Ego, A. Kaida, M. Matsumoto, P. P. Pandolfi, and K. Shimotohno.** 2003. Distinct nuclear body components, PML and SMRT, regulate the *trans*-acting function of HTLV-1 Tax oncoprotein. Oncogene **22**:1611–1619.
4. **Ariumi, Y., P. Turelli, M. Masutani, and D. Trono.** 2005. DNA damage sensors ATM, ATR, DNA-PKcs, and PARP-1 are dispensable for human immunodeficiency virus type 1 integration. J. Virol. **79**:2973–2978.
5. **Bridge, A. J., S. Pebernard, A. Ducraux, A.-L. Nicoulaz, and R. Iggo.** 2003. Induction of an interferon response by RNAi vectors in mammalian cells. Nat. Genet. **34**:263–264.
6. **Brummelkamp, T. R., R. Bernard, and R. Agami.** 2002. A system for stable expression of short interfering RNAs in mammalian cells. Science **296**:550–553.
7. **Chang, P. C., C. W. Chi, G. Y. Chau, F. Y. Li, Y. H. Tsai, J. C. Wu, and Y. H. Lee.** 2006. DDX3, a DEAD box RNA helicase, is deregulated in hepatitis virus-associated hepatocellular carcinoma and is involved in cell growth control. Oncogene **25**:1991–2003.
8. **Chao, C. H., C. M. Chen, P. L. Cheng, J. W. Shih, A. P. Tsou, and Y. H. Lee.** 2006. DDX3, a DEAD box RNA helicase with tumor growth-suppressive property and transcriptional regulation activity of the $p21^{waf1/cip1}$ promoter, is a candidate tumor suppressor. Cancer Res. **66**:6579–6588.
9. **Cordin, O., J. Banroques, N. K. Tanner, and P. Linder.** 2006. The DEAD-box protein family of RNA helicases. Gene **367**:17–37.
10. **Fang, J., S. Kubota, B. Yang, N. Zhou, H. Zang, R. Godbout, and R. J. Pomerantz.** 2004. A DEAD box protein facilitates HIV-1 replication as a cellular co-factor of Rev. Virology **330**:471–480.
11. **Goh, P. Y., Y. J. Tan, S. P. Lim, Y. H. Tan, S. G. Lim, F. Fuller-Pace, and W. Hong.** 2004. Cellular RNA helicase p68 relocalization and interaction with the hepatitis C virus (HCV) NS5B protein and the potential role of p68 in HCV RNA replication. J. Virol. **78**:5288–5298.
12. **Huang, H., M. L. Shiffman, R. C. Cheung, T. J. Layden, S. Friedman, O. T. Abar, L. Yee, A. P. Chokkalingam, S. J. Schrodi, J. Chan, J. J. Catanese, D. U. Leong, D. Ross, X. Hu, A. Monto, L. B. McAllister, S. Broder, T. White, J. J. Sninsky, and T. L. Wright.** 2006. Identification of two gene variants associated with risk of advanced fibrosis in patients with chronic hepatitis C. Gastroenterology **130**:1679–1687.
13. **Ikeda, M., K. Abe, H. Dansako, T. Nakamura, K. Naka, and N. Kato.** 2005. Efficient replication of a full-length hepatitis C virus genome, strain O, in cell culture, and development of a luciferase reporter system. Biochem. Biophys. Res. Commun. **329**:1350–1359.
14. **Kato, N., K. Sugiyama, K. Namba, H. Dansako, T. Nakamura, M. Takami,**

K. Naka, A. Nozaki, and K. Shimotohno. 2003. Establishment of a hepatitis C virus subgenomic replicon derived from human hepatocytes infected in vitro. Biochem. Biophys. Res. Commun. **306**:756–766.
15. **Kwong, A. D., B. G. Rao, and K. T. Jeang.** 2005. Viral and cellular RNA helicases as antiviral targets. Nat. Rev. Drug Discov. **4**:845–853.
16. **Lohmann, V., F. Körner, J.-O. Koch, U. Herian, L. Theilman, and R. Bartenschlager.** 1999. Replication of subgenomic hepatitis C virus RNAs in a hepatoma cell line. Science **285**:110–113.
17. **Mamiya, N., and H. J. Worman.** 1999. Hepatitis C virus core protein binds to a DEAD box RNA helicase. J. Biol. Chem. **274**:15751–15756.
18. **Naldini, L., U. Blömer, P. Gallay, D. Ory, R. Mulligan, F. H. Gage, I. M. Verma, and D. Trono.** 1996. In vivo gene delivery and stable transduction of non-dividing cells by a lentiviral vector. Science **272**:263–267.
19. **Owsianka, A. M., and A. H. Patel.** 1999. Hepatitis C virus core protein interacts with a human DEAD box protein DDX3. Virology **257**:330–340.
20. **Rocak, S., and P. Linder.** 2004. DEAD-box proteins: the driving forces behind RNA metabolism. Nat. Rev. Mol. Cell Biol. **5**:232–241.
21. **Sato, S., M. Fukasawa, Y. Yamakawa, T. Natsume, T. Suzuki, I. Shoji, H. Aizaki, T. Miyamura, and M. Nishijima.** 2006. Proteomic profiling of lipid droplet proteins in hepatoma cell lines expressing hepatitis C virus core protein. J. Biochem. **139**:921–930.
22. **Tingting, P., F. Caiyun, Y. Zhigang, Y. Pengyuan, and Y. Zhenghong.** 2006. Subproteomic analysis of the cellular proteins associated with the 3′ untranslated region of the hepatitis C virus genome in human liver cells. Biochem. Biophys. Res. Commun. **347**:683–691.
23. **Wakita, T., T. Pietschmann, T. Kato, T. Date, M. Miyamoto, Z. Zhao, K. Murthy, A. Habermann, H. G. Kräusslich, M. Mizokami, R. Bartenschlager, and T. J. Liang.** 2005. Production of infectious hepatitis C virus in tissue culture from a cloned viral genome. Nat. Med. **11**:791–796.
24. **Yedavalli, V. S., C. Neuveut, Y. H. Chi, L. Kleiman, and K. T. Jeang.** 2004. Requirement of DDX3 DEAD box RNA helicase for HIV-1 Rev-RRE export function. Cell **119**:381–392.
25. **You, L. R., C. M. Chen, T. S. Yeh, T. Y. Tsai, R. T. Mai, C. H. Lin, and Y. H. Lee.** 1999. Hepatitis C virus core protein interacts with cellular putative RNA helicase. J. Virol. **73**:2841–2853.
26. **Zufferey, R., D. Nagy, R. J. Mandel, L. Naldini, and D. Trono.** 1997. Multiply attenuated lentiviral vector achieves efficient gene delivery in vivo. Nat. Biotechnol. **15**:871–875.

nature
cell biology

The lipid droplet is an important organelle for hepatitis C virus production

Yusuke Miyanari[1,2], Kimie Atsuzawa[3], Nobuteru Usuda[3], Koichi Watashi[1,2], Takayuki Hishiki[1,2], Margarita Zayas[4], Ralf Bartenschlager[4], Takaji Wakita[5], Makoto Hijikata[1,2] and Kunitada Shimotohno[1,2,6]

The lipid droplet (LD) is an organelle that is used for the storage of neutral lipids. It dynamically moves through the cytoplasm, interacting with other organelles, including the endoplasmic reticulum (ER)[1-3]. These interactions are thought to facilitate the transport of lipids and proteins to other organelles. The hepatitis C virus (HCV) is a causative agent of chronic liver diseases[4]. HCV capsid protein (Core) associates with the LD[5], envelope proteins E1 and E2 reside in the ER lumen[6], and the viral replicase is assumed to localize on ER-derived membranes. How and where HCV particles are assembled, however, is poorly understood. Here, we show that the LD is involved in the production of infectious virus particles. We demonstrate that Core recruits nonstructural (NS) proteins and replication complexes to LD-associated membranes, and that this recruitment is critical for producing infectious viruses. Furthermore, virus particles were observed in close proximity to LDs, indicating that some steps of virus assembly take place around LDs. This study reveals a novel function of LDs in the assembly of infectious HCV and provides a new perspective on how viruses usurp cellular functions.

Hepatitis C virus (HCV) has a plus-strand RNA genome that encodes the viral structural proteins Core, E1 and E2, the p7, and the nonstructural (NS) proteins 2, 3, 4A, 4B, 5A and 5B (refs 7, 8). NS proteins are reported to localize on the cytoplasmic side of endoplasmic reticulum (ER) membranes[9]. To elucidate the mechanisms of virus production, we used a HCV strain, JFH1, which can produce infectious viruses[10-12]. We first investigated the subcellular localization of the HCV proteins in cells that had been transfected with JFH1^{E2FL} RNA, in which a part of the hypervariable region 1 of E2 was replaced by the FLAG epitope tag (see Supplementary Information, Fig. S1, S2a–d). Core localized to the lipid droplets (LDs; Fig. 1a), as previously reported[5]. Interestingly, NS proteins were also detected around LDs in 60–90% of JFH1^{E2FL}-replicating cells (Fig. 1a, c). Similar levels of colocalization of LDs with viral proteins were observed in cells that had been transfected with chimeric HCV genomes expressing structural proteins, p7 and part of NS2 of the genotype 1b (Con1) or the genotype 1a (H77) isolate (see Supplementary Information, Fig. S1, S2e)[13]. In contrast, there was no close association between the LDs and NS proteins in cells that had been transfected with JFH1^{dC3} RNA (Fig. 1b, c), which lacked the coding region of Core (Supplementary Information, Fig. S1). NS proteins were diffusely present on the ER, suggesting that NS proteins are translocated from the ER to LDs in JFH1^{E2FL}-replicating cells in a Core-dependent manner. Importantly, there was no association between LDs and PDI, an ER marker protein, indicating that either ER membranes were absent in close proximity to LDs or that PDI was excluded from such membranes (Fig. 1c). These results were supported by western blot analysis of the LD fraction (Fig. 1d). The LD fraction contained ADRP, an LD marker, but not the ER markers Calnexin and Grp78 (data not shown), indicating that there was no ER contamination in the LD fraction. However, the LD fraction from JFH1^{E2FL}-replicating cells contained high levels of viral proteins in contrast to the LD fraction from JFH1^{dC3}-replicating cells (in which HCV proteins were virtually absent (Fig. 1d, LD fraction)), even though the expression levels of the NS proteins in whole-cell extracts were similar (Fig. 1d, whole-cell extract). About 20–45% of the total HCV proteins associated with the LDs in JFH1^{E2FL}-replicating cells (Fig. 1e). Consistent with previous reports that Core enhances the formation of LDs[14], overproduction of LDs was observed in JFH1^{E2FL}-, but not JFH1^{dC3}-replicating cells (Supplementary Information, Fig. S3a–l). Treatment of the cells with oleic acid, which enhanced the formation of LDs, did not affect either HCV protein levels or the recruitment of viral proteins to LDs in JFH1^{dC3}-replicating cells (Supplementary Information, Fig. S3m–p). Thus, the overproduction of LDs is insufficient for the recruitment of HCV proteins to LDs. To examine the ability of Core to recruit NS proteins to LDs, JFH1^{dC3}-replicating cells were transfected with a plasmid-expressing Core (Core^{WT}) (Fig. 1f, g). NS5A accumulated around LDs (Fig. 1f, arrowheads and panel 2), as did NS3 and NS4AB (Fig. 1g), in cells expressing Core^{WT}. The translocation of NS proteins to LDs was, however, not observed in JFH1^{dC3}-replicating cells expressing Core$^{PP/AA}$ (Fig. 1g and Supplementary Information, Fig. S2f–h),

[1]Department of Viral Oncology, Institute for Virus Research, Kyoto University, Kyoto 606-8507, Japan; [2]Graduate School of Biostudies, Kyoto University, Kyoto 606-8507, Japan; [3]Department of Anatomy, Fujita Health University School of Medicine, Toyoake 470-1192, Japan; [4]Department of Molecular Virology, University of Heidelberg, 69120 Heidelberg, Germany; [5]Department of Virology II, National Institute of Infectious Diseases, Tokyo 162-8640, Japan
[6]Correspondence should be addressed to K.S. (e-mail: shimkuni@z8.keio.jp)

Received 16 March 2007; accepted 31 July 2007; published online 26 August 2007; DOI: 10.1038/ncb1631

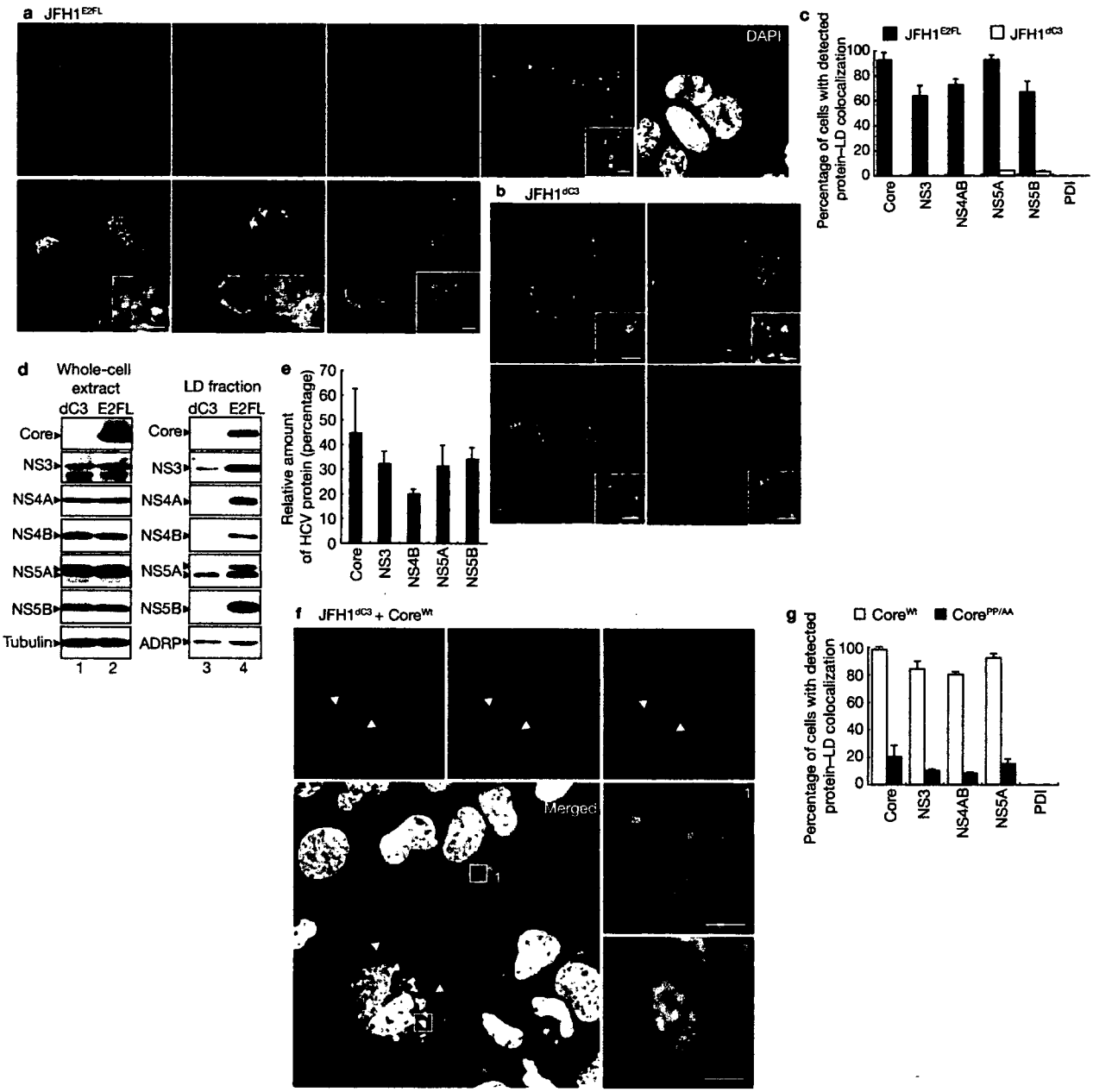

Figure 1 Core recruits NS proteins to LDs. (**a**) Huh-7 cells transfected with JFH1^{E2FL} RNA were labelled with antibodies against Core (red), NS5A (blue), NS3 (red), NS4AB (red) or NS5B (red). Lipid droplets (LDs) and nuclei were stained with BODYPI 493/503 (green) and DAPI (white in upper panel, blue in lower panels), respectively. Insets are high magnification images of areas in the respective panel. (**b**) JFH1^{dC3} replicon-bearing cells were labelled with DAPI (blue), BODIPY 493/503 (green) and indicated antibodies (red). The insets are high magnifications of the corresponding panel. (**c**) Percentages of JFH1^{E2FL}- or JFH1^{dC3}-bearing cells in which hepatitis C virus (HCV) proteins or PDI colocalize with LDs ($n > 200$). (**d**) Western blot analysis of HCV proteins and marker proteins in whole-cell extracts and the LD fractions from cells transfected with JFH1^{E2FL} (E2FL) or JFH1^{dC3} (dC3) RNA. (**e**) HCV proteins were quantified by using western blotting data of the purified LD fraction and whole-cell extracts of JFH1^{E2FL}-replicating cells. Results are shown as relative amounts of HCV proteins co-fractionated with LDs. This results correspond well with results obtained by quantitative immunofluorescence staining (data not shown). (**f**) Trans-complementation with Core^{Wt} relocates NS proteins to LDs. JFH1^{dC3} replicon-bearing cells were transfected with pcDNA3–Core^{Wt} and labelled with BODIPY 493/503 (green), DAPI (white) and antibodies against NS5A (red) and Core (blue). Arrowheads indicate Core^{Wt}-expressing cells. Higher-magnification images of area 1 and area 2 are shown in panels 1 and 2, respectively. Scale bars, 2 μm. (**g**) The percentages of cells in which HCV proteins colocalize with LDs in the presence of Core^{Wt} or Core $^{PP/AA}$ ($n > 200$). Uncropped images of gels are shown in Supplementary Information Fig. S6. All error bars are derived from s.d.

a variant of Core containing two alanine substitutions at amino-acid positions 138 and 143 that fails to associate with LDs[15]. These results show that LD-associated Core recruits NS proteins from the ER to LDs.

Next, we investigated whether Core also recruited HCV RNA to LDs. *In situ* hybridization analysis showed that in more than 80% of JFH1^{E2FL}-replicating cells, both plus- and minus-strand RNAs were diffusely

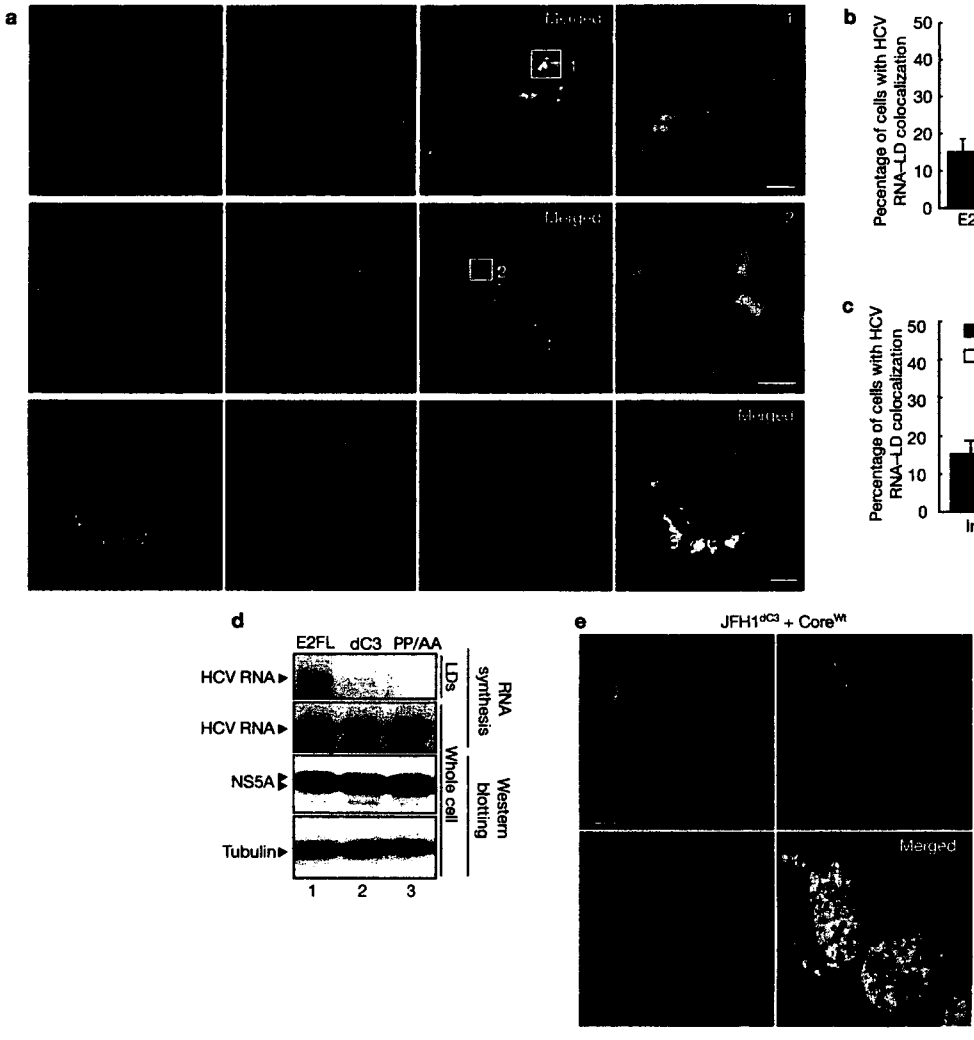

Figure 2 Core-dependent recruitment of active HCV replication complexes to the LD. (**a**) Huh-7 cells transfected with JFH1^{E2FL} RNA were analysed by *in situ* hybridization with strand-specific probes (plus or minus). The cells were labelled to simultaneously visualize lipid droplets (LDs), NS5A and Core (lower panels). Higher-magnification images of area 1 and area 2 are shown in the upper and middle right panels 1 and 2, respectively. Scale bars: 2 μm (panels 1, 2); 10 μm (lower right panel). (**b**) The percentages of JFH1^{E2FL}-, JFH1^{dC3}- and JFH1$^{PP/AA}$-expressing cells positive for overlapping signals for LDs and plus- or minus-strand hepatitis C virus (HCV) RNA ($n > 200$). (**c**) Intact or digitonin and nuclease-treated (dig/nuc) JFH1^{E2FL} replicon-bearing cells were analysed by *in situ* hybridization. The percentages of cells with overlapping signals for LD and plus- or minus-strand HCV RNA are shown ($n > 200$). (**d**) RNA-synthesizing activity in the LD fractions purified from cells transfected with JFH1^{E2FL}, JFH1^{dC3} or JFH1$^{PP/AA}$ RNA (top panel). As a control, HCV RNA synthesis activity in digitonin-permeabilized cells was analysed (second panel from the top). HCV protein levels represented by NS5A are shown, together with the level of tubulin (bottom two panels). (**e**) Localization of plus-strand HCV RNA and Core in JFH1^{dC3} replicon-bearing cells transfected with pcDNA3–Core^{Wt} (Scale bar, 10 μm). Uncropped images of gels are shown in Supplementary Information Fig. S6. All error bars are derived from s.d.

located in the perinuclear region (see Supplementary Information, Fig. S4a). More importantly, in about 20% of these cells, plus- and minus-strand RNAs accumulated around LDs (Fig. 2a, upper and middle panels; 2b) and colocalized with HCV proteins such as Core and NS5A (Fig. 2a, lower panels). No association between HCV RNA and LDs was detected in JFH1^{dC3}- or JFH1$^{PP/AA}$-replicating cells (Fig. 2b). Northern blot analysis revealed that 4.8% and 5.4% of total plus- and minus-strand HCV RNA, respectively, were detected in purified LD fractions of JFH^{E2FL}-replicating cells (data not shown). Induction of LD formation with oleic acid did not affect HCV RNA accumulation around LDs (data not shown). These results provide strong evidence that Core recruits HCV RNA as well as NS proteins to LDs.

The HCV replication complex is compartmentalized by lipid bilayer membranes[16–18]. Therefore, HCV RNA in the complex is resistant to nuclease treatment in digitonin-permeabilized cells[17] (Supplementary Information, Fig. S4b–d). *In situ* hybridization analysis did not reveal a significant difference in the number of cells containing LD-associated HCV RNA before and after nuclease treatment (Fig. 2c), indicating that HCV RNA around LDs is part of the replication complex. An RNA synthesis assay showed that the purified LD fraction from JFH1^{E2FL}-, but not JFH1^{dC3}- or JFH1$^{PP/AA}$-replicating cells, possessed HCV RNA synthesis activity, even though the expression levels of viral proteins and RNA-synthesizing activities in total cell lysates were similar (Fig. 2d). Moreover, the addition of Core^{Wt} rescued the localization of plus- and minus-strand

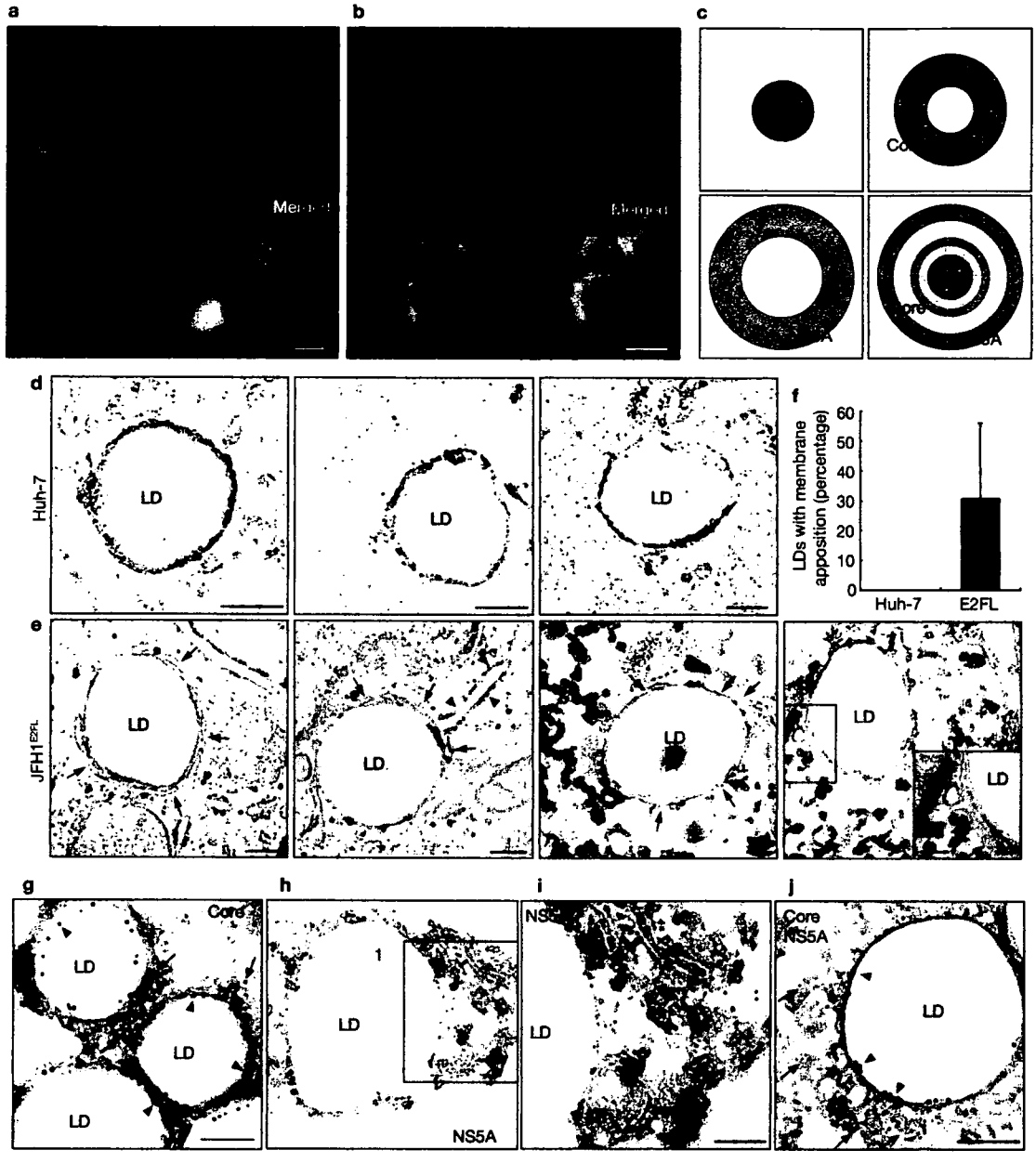

Figure 3 Spatial distribution of Core and NS5A relative to the LD. (**a**, **b**) The localizations of Core, NS5A and ADRP around the lipid droplets (LDs) in JFH1^{E2FL} replicon-bearing cells were analysed using immunofluorescence microscopy. Scale bars, 1 μm. (**c**) Typical images of the localization of LDs, Core, NS5A and merged images are shown with the relative scale of each image. (**d**, **e**) Transmission electron micrographs of LDs in naïve Huh-7 cells and JFH1^{E2FL}-expressing cells. Arrows and arrowheads indicate LD-associated membranes and rough ER membranes, respectively. (**f**) Frequency of LDs with close appositions of membrane cisternae. About 100 Huh-7 cells or JFH1^{E2FL}-expressing cells, respectively, were chosen randomly. LDs with apposed membrane cisternae, as exemplified in panel **e**, were counted as positive. The LDs judged as positive were divided by the total number of LDs. (**g**–**j**) Immunoelectron micrographs of LDs labelled with antibodies against Core (**g**), NS5A (**h**, **i**) or both (**j**) are shown. Panel **i** is a higher magnification of area 1 in panel **h**. In panel **j**, Core and NS5A are labelled with 15 nm and 10 nm gold particles, respectively. Scale bars, 200 nm. All error bars are derived from s.d.

HCV RNA around LDs in JFH^{dC3}-replicating cells (Fig. 2e and data not shown). Both plus- and minus-strand RNA associated with LDs were nuclease resistant (data not shown). These results demonstrate that Core recruits biologically active replication complexes to LDs.

The LD is surrounded by a phospholipid monolayer[19], whereas HCV replication complexes are likely to be surrounded by lipid bilayer membranes[16,17]. Therefore, the replication complexes might not be directly associated with the membranes of LDs. To characterize the colocalization of LDs, viral proteins and replication complexes more precisely, we analysed the localization of NS5A with high-resolution immunofluorescence microscopy. Core was completely colocalized with ADRP, residing on the surface of LDs[20] (Fig. 3a), thus indicating that Core also directly associates with the surface of LDs. More importantly, NS5A mainly localized around the Core-positive area, resulting in a doughnut-shaped signal with a diameter slightly

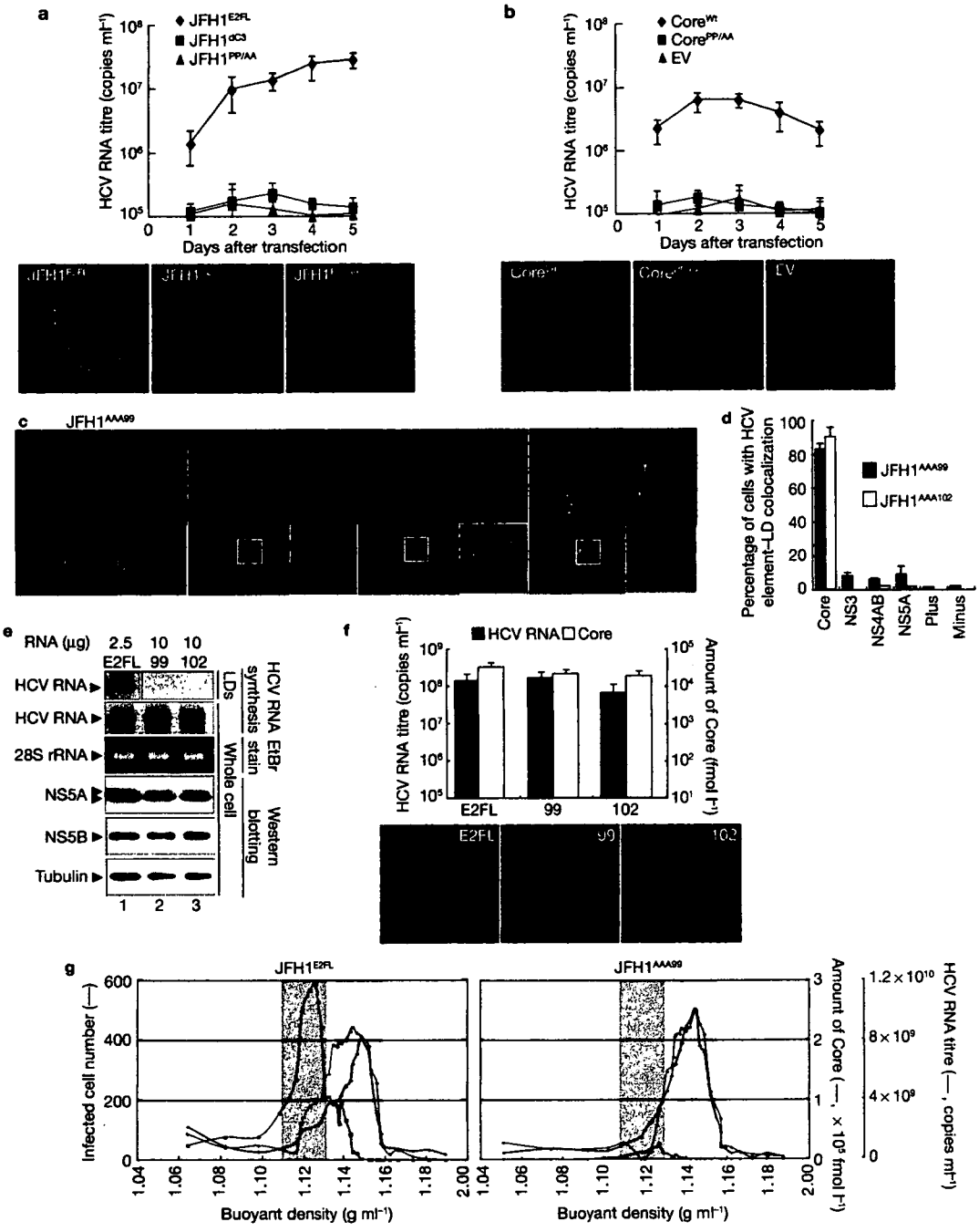

Figure 4 LD associations of Core and NS proteins are necessary for the production of infectious HCV particles. (**a**) The culture medium from JFH1^{E2FL}-, JFH1^{dC3}- or JFH1$^{PP/AA}$-replicating cells was collected at the indicated time points and the titre of hepatitis C virus (HCV) RNA was measured by real-time RT-PCR (upper panel, $n = 3$). The culture medium was added to naïve Huh7.5 cells and, 24 h after inoculation, and cells were labelled with anti-HCV antibodies (lower panels, red). (**b**) JFH1^{dC3} replicon-bearing cells were transfected with pcDNA3 (EV), pcDNA3–Core^{Wt} (Core^{Wt}) or pcDNA3–Core$^{PP/AA}$ (Core$^{PP/AA}$). The level of HCV RNA and the infectivity of the culture medium were examined as described above ($n = 3$). (**c**) Subcellular localization of NS5A and Core in cells expressing JFH1^{AAA99}. The insets are high magnifications of the area of the corresponding panel. Scale bar, 2 μm. (**d**) Percentages of cells in which the signals for given HCV proteins, and plus- and minus-strand HCV RNA, overlapped with those for LDs ($n > 200$). (**e**) Different amounts of JFH1^{E2FL} (E2FL), JFH1^{AAA99} (99) or JFH1^{AAA102} (102) RNAs, respectively, were transfected into the same number of Huh-7 cells. HCV RNA synthesis activity in purified LD fractions (LD) and whole-cell lysates (whole cell) was analysed (HCV RNA synthesis). 28S rRNA was used as a control. Western blot analysis of NS5A, NS5B and tubulin in cells is also shown. All the RNA samples in the top panel were run on the same gel. (**f**) Analysis of HCV released from cells expressing JFH1^{E2FL}, JFH1^{AAA99} or JFH1^{AAA102}. HCV RNA titres (black bars) and amounts of Core (white bars) accumulated in the culture medium at 5 d after RNA transfection were measured (upper panel, $n = 3$). Infectivity of the culture medium for naïve Huh-7.5 cells was analysed as described above (lower panels). (**g**) Concentrated culture medium from JFH1^{E2FL}- and JFH1^{AAA99}-replicating cells was fractionated using 20–50% sucrose density-gradient centrifugation at 100,000 *g* for 16 h. For each fraction, the amounts of Core (black line), HCV RNA (blue line) and infectivity (represented by infected cell numbers in a well; red line) are plotted against the buoyant density (*x*-axis) ($n = 3$). Uncropped images of gels are shown in Supplementary Information Fig. S6. All error bars are derived from s.d.

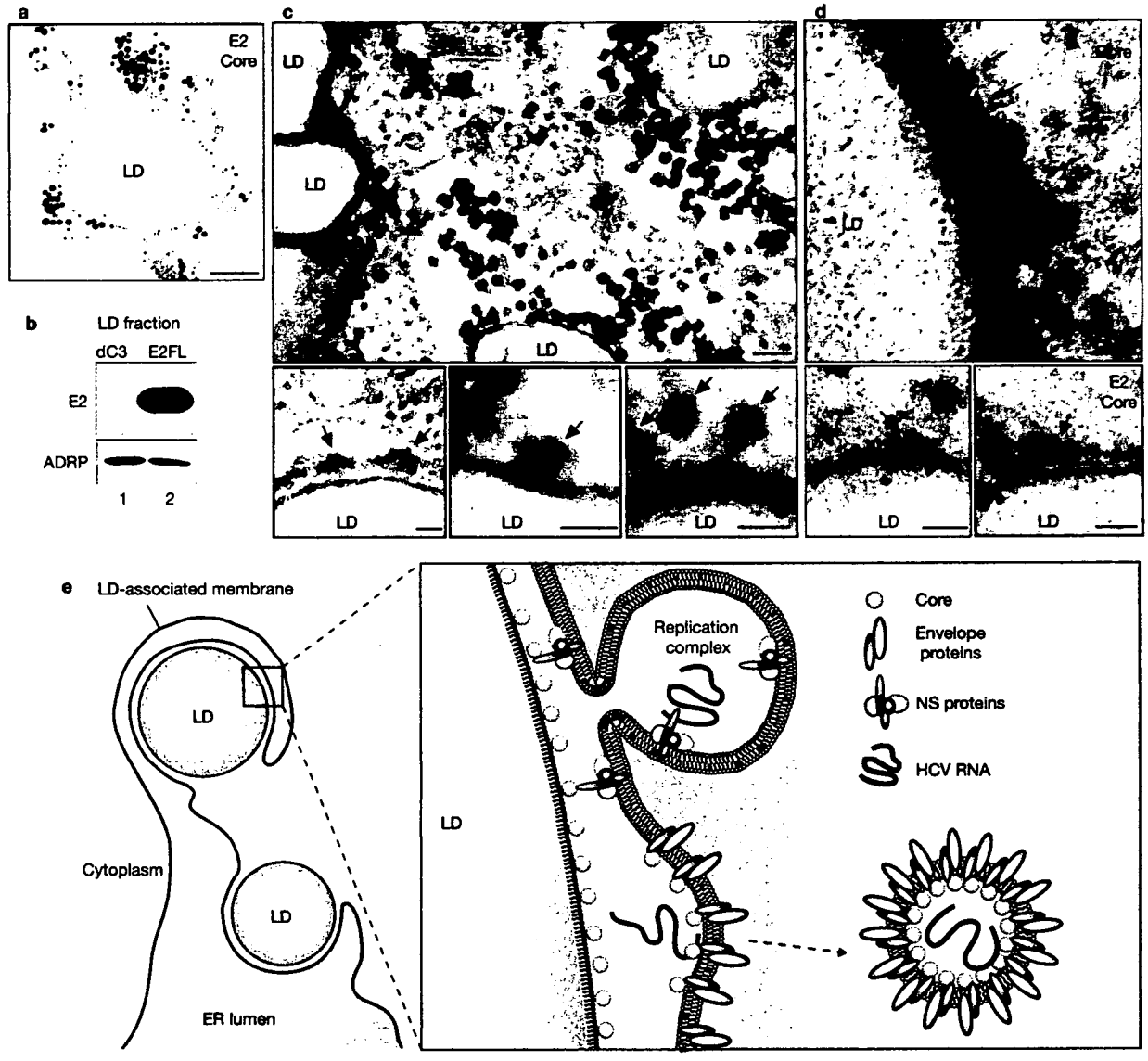

Figure 5 Virus-assembly takes place around the LDs. (**a**) Immunoelectron microscopic detection of E2 and Core in JFH1^{E2FL}-replicating cells. E2 and Core are labelled with 15 nm and 10 nm gold particles, respectively. (**b**) Western blot analysis of the lipid droplet (LD) fraction from JFH1^{E2FL} and JFH1^{dC3} replicon-bearing cells with anti-E2 and anti-ADRP antibodies. (**c**) Transmission electron micrographs of JFH1^{E2FL}-replicating cells. Arrows indicate virus-like particles. (**d**) Immunoelectron micrographs of LDs labelled with antibodies against Core (10 nm) and E2 (15 nm) are shown. Arrows show Core in electron-dense granules. Scale bar: **a** and upper panel of **c**: 100 nm; in **d** and lower panels of **c**: 50 nm. (**e**) A model for the production of infectious hepatitis C virus (HCV). Core mainly localizes on the monolayer membrane that surrounds the LD. HCV induces the apposition of the LD to the endoplasmic reticulum (ER)-derived bilayer membranes (LD-associated membrane). Core recruits NS proteins, as well as replication complexes, to the LD-associated membrane. NS proteins around the LD can then participate in infectious virus production. E2 also localizes around the LD. Through these associations, virion assembly proceeds in this local environment. Uncropped images of gels are shown in Supplementary Information Fig. S6.

larger than that of Core (Fig. 3b). The LD-proximal NS5A signal partially overlapped with the Core signal (Fig. 3b, c, grey). This concentric staining pattern was also observed with the other NS proteins (Supplementary Information, Fig. S5a), indicating that NS proteins associate with Core on the surface of LDs. Electron microscopic analysis only rarely revealed a close association of LDs with other organelles in naïve Huh-7 cells (Fig. 3d, f). However, in the case of JFH1^{E2FL}-replicating cells, about 30% of the LDs were in close proximity to membrane cisternae (Fig. 3e, arrows; 3f), arguing for a HCV-induced membrane rearrangement around LDs. Core was mainly located on the periphery of LDs, and occasionally signals were observed in more distal areas of the LDs (Fig. 3g, arrowheads and arrows, respectively). Although some NS5A signals were observed on the surface of the LD, the majority of NS5A signals were detected more distal of LDs (Fig. 3h, i). Furthermore, we often observed membrane cisternae as white lines in the same area as NS5A signals (Fig. 3i, arrows). When the same section was labelled with anti-Core and anti-NS5A antibodies, Core was detected on the surface of the LDs, whereas NS5A was mainly observed in the peripheral area of the LDs (Fig. 3j, arrowheads and arrows, respectively). In summary, these results show that Core recruits NS proteins, as well as HCV replication complexes, to the LD-associated membranes.

The above results prompted us to ask whether Core–LD colocalization is important for the production of infectious virus particles. JFH1^{E2FL}-replicating cells released virions into the culture medium and these viruses were highly infectious for naïve Huh-7.5 cells[11,21], although culture medium from JFH1$^{PP/AA}$- or JFH1^{dC3}-replicating cells did not contain significant levels of HCV RNA and infectious virus (Fig. 4a). However, following trans-complementation with Core^{Wt}, a high titre of HCV RNA and infectious virus could be rescued from JFH1^{dC3}-replicating cells (Fig. 4b; and see Supplementary Information, Fig. S5b, c). In contrast, the production of infectious viruses was not rescued by trans-complementation with Core$^{PP/AA}$ (Fig. 4b). RNA-binding properties and oligomerization of Core^{Wt} and Core$^{PP/AA}$, which are both necessary for virus assembly, were similar (Supplementary Information, Fig. S5d; ref. 22), arguing that the primary defect of this mutant in preventing infectious virus production is the inability to associate with LDs.

To investigate the contribution of NS proteins around LDs to infectious virus production, we used variants of NS5A, which were not recruited to LDs even in the presence of Core. We assumed that NS5A was crucial for recruiting other NS proteins to LDs, because the level of NS5A recruited to LDs via Core was higher than the levels of the other recruited NS proteins (Fig. 1c, JFH1^{E2FL}). Using alanine-scanning mutagenesis within the NS5A coding region of JFH1^{E2FL}, we generated two mutants, JFH1^{AAA99} and JFH1^{AAA102}, in which the amino-acid sequence APK (aa 99–101 of NS5A) or PPT (aa 102–104 of NS5A) was replaced by AAA (Supplementary Information, Fig. S1). In JFH1^{AAA99}- and JFH1^{AAA102}-replicating cells, NS5A was rarely detected around LDs, whereas Core was still localized to LDs (Fig. 4c, d). Importantly, these mutations impaired not only the NS5A association with LDs, but also the recruitment of other NS proteins and viral RNAs to LDs (Fig. 4d). These results indicate that NS5A is a key protein that recruits replication complexes to LDs. Importantly, HCV RNA synthesis activity in the LD fractions from these mutant JFH1-replicating cells was also severely impaired (Fig. 4e), corroborating the lack of association of HCV replication complexes with LDs.

To investigate the infectious virus production of these NS5A mutants, we prepared cells expressing similar levels of HCV proteins and RNA by adjusting the amount of transfected HCV RNA (Fig. 4e). This was necessary, because replication activities of these mutants were lower compared with JFH1^{E2FL}. Under these conditions, the amounts of Core and HCV RNA that were released into the culture medium from cells transfected with the mutants were comparable to JFH^{E2FL} (Fig. 4f, upper graph). However, infectivity titres of the mutants were severely reduced (Fig. 4f, lower panels). In sucrose density-gradient centrifugation of culture medium from JFH1^{E2FL}-bearing cells, two types of HCV particles were detected: low-density particles (about 1.12 g ml^{-1}) with high infectivity (Fig. 4g, green area of JFH1^{E2FL}), and high-density particles (about 1.15 g ml^{-1}) without infectivity (yellow area). This result indicates that only a minor portion of released HCV particles is infectious, whereas the majority of released particles lack infectivity. In contrast, cells bearing the JFH1^{AAA99} mutant almost exclusively released non-infectious particles of around 1.15 g ml^{-1}, whereas infectious particles were barely detectable (Fig. 4g, JFH1^{AAA99}). Taken together, these results provide convincing evidence that the association of NS proteins and replication complexes around LDs is critical for producing infectious viruses, whereas production of non-infectious viruses seems to follow a different pathway.

The results described so far imply that some step(s) of HCV assembly take place around LDs. To explore this possibility, we analysed the distribution of the major envelope protein E2 around the LD. Electron microscopic analysis revealed that, in about 90% of JFH1^{E2FL}-replicating cells, E2 was localized in the peripheral area of the LDs (Fig. 5a, large grains). This labelling pattern was similar to the one observed for NS5A (Fig. 3j), indicating that E2 also localizes on the LD-associated membranes. Western blot analysis of the LD fraction supported this conclusion, because the LD fraction that was purified from JFH1^{E2FL}-replicating cells, but not from JFH1^{dC3}-replicating cells, contained E2 (Fig. 5b). Furthermore, spherical virus-like particles with an average diameter of about 50 nm were observed around LDs in JFH1^{E2FL}-replicating cells (Fig. 5c, upper panel). These particles were never observed in naïve Huh-7 cells. A more refined analysis indicates that these particles are closely associated with membranes in close proximity to LDs (Fig. 5c, lower panels, arrows). Finally, these particles around the LDs reacted with Core- and E2-specific antibodies, arguing that the particles represent true HCV virions (Fig. 5d). These results suggest that infectious HCV particles are generated from the LD-associated membranous environment.

In this study, we have demonstrated that Core recruits NS proteins, HCV RNAs and the replication complex to LD-associated membranes. Mutations of Core and NS5A (Fig. 4), which failed to associate with LDs, impaired the production of infectious virus. We note that the mutant Core retains the ability to interact with RNA (Supplementary Information, Fig. S5b) and to assemble into nucleocapside[22]. Similarly, the NS5A mutant still supports viral genome replication and the formation of capsids or virus-like particles, arguing that the introduced mutations in Core and NS5A do not affect overall protein folding, stability or function (Fig. 4). Taken together, the data show that the association of HCV proteins with LDs is important for the production of infectious viral particles (Fig. 5e).

Our results also indicate that NS proteins around the LDs participate in the assembly of infectious virus particles. In one scenario, NS proteins may indirectly contribute to the different steps of virus production — for example, by establishing the microenvironment around the LDs that is required for infectious virus production. Alternatively, NS proteins around the LDs may directly participate in virus production — for example, as components of the replication complex that provide the RNA genome to the assembling nucleocapsid.

In support of the role of LDs in virus formation, we observed that colocalization of HCV protein with LDs was low in cases of the chimera Jc1, supporting up to 1,000-fold higher infectivity titres compared with JFH1 (ref. 13). In a Jc1-infected cell, only about 20% of LDs demonstrated detectable colocalization with Core, but this value increased to 80% in the case of a Jc1 mutant lacking most of the envelope glycoprotein genes and thus being unable to produce infectious virus particles (data not shown). This inverse correlation between the efficiency of virus production and Core protein accumulation on LDs indicates that rapid assembly and virus release results in the rapid liberation of HCV proteins from the LDs.

Steatosis and abnormal lipid metabolism caused by chronic HCV infection may be linked to enhanced LD formation[14]. In fact, the overproduction of LDs is induced by Core (Supplementary Information, Fig. S3) and HCV also induces membrane rearrangements around LDs (Fig. 3d–f). Our findings suggest that excessive Core-dependent formation of LDs

and membrane rearrangements are required to supply the necessary microenvironment for virus production. NS proteins and HCV RNA seem to be translocated from the ER to the LD-associated membranes. Interestingly, the LD-associated membranes were occasionally found in continuity with ribosome-studded rough ER (Fig. 3e, arrowheads). Thus, at least parts of the LD-associated membranes are likely to be derived from ER membranes. ER marker proteins, however, were not detected in the LD fraction, suggesting that the LD-associated membrane is characteristically distinct from that of ER membranes.

To our knowledge, this is the first report showing that LDs are required for the formation of infectious virus particles. The fact that capsid protein of the hepatitis G virus also localizes to LDs[15] indicates that LDs might be important for the production of other viruses as well. Our findings demonstrate a novel function of LDs, provide an important step towards elucidating the mechanism of HCV virion production and open new avenues for novel antiviral intervention. □

METHODS

Antibodies. The antibodies used for immunoblotting and immunolabelling were specific for Core (#32-1 and RR8); E2 (AP-33 (ref. 23); 3/11, CBH5 and Flag M2 (Sigma-Aldrich, St Louis, MO); NS3 (R212)[17]; NS4A and 4B (PR12); NS5A (NS5ACL1); NS5B (NS5B-6 and JFH1-1)[24]; ADRP (Progen Biotechnik, Heidelberg, Germany); tubulin (Oncogene Research Products, MA, USA); Grp78 (StressGen, Victoria, Canada); PDI (StressGen); and Calnexin-NT (StressGen). Antibodies specific for Core (#32-1 and RR8), NS3 (R212) and NS4AB (PR12) were gifts from Dr Kohara (The Tokyo Metropolitan Institute of Medical Science, Japan). Anti-E2 antibody (AP-33) was provided by Dr Patel (MRC Virology Unit, UK). Anti-NS5B (NS5B-6) antibody was kindly provided by Dr Fukuya (Osaka University, Japan). Rabbit polyclonal antibodies specific for NS5A were raised against a bacterially expressed GST-NS5A (1–406 aa) fusion protein. In the case of the HCV chimeras Con1/C3 and H77/C3, immunofluorescence analyses were performed by using the following antibodies: Core (C7/50)[5], a JFH1 NS3-specific rabbit polyclonal antiserum; NS4B (#86)[25]; and NS5A (Austral Biologicals, San Ramon, CA).

Indirect immunofluorescence analysis. Indirect immunofluorescence analysis was performed essentially as described previously[17], with slight modifications. Cells transfected with JFH1 RNA were seeded onto a collagen-coated Labtech II 8-well chamber (Nunc, NY, USA). The coating with collagen was performed using rat-tail collagen type I (BD Bioscience, Palo Alto, CA) according to manufacturer's instructions. Three days after seeding, the cells were washed twice with phosphate-buffered saline (PBS; 137 mM NaCl, 2.7 mM KCl, 4.3 mM Na_2HPO_4 and 1.4 mM KH_2PO_4) and fixed with fixation solution (4% paraformaldehyde and 0.15 M sodium cacodylate at pH 7.4) for 15 min at room temperature. After washing with PBS, the cells were permeabilized with 0.05% Triton X-100 in PBS for 15 min at room temperature. For the precise localization of the proteins, the cells were permeabilized with 50 μg ml^{-1} of digitonin in PBS for 5 min at room temperature[26]. After incubating the cells with blocking solution (10% fetal bovine serum and 5% bovine serum albumin (BSA) in PBS) for 30 min, the cells were incubated with the primary antibodies. The fluorescent secondary antibodies were Alexa 568- or Alexa 647-conjugated anti-mouse or anti-rabbit IgG antibodies (Invitrogen, Carlsbad, CA). Nuclei were labelled with 4',6-diamidino-2-phenylindole (DAPI). LDs were visualized with BODIPY 493/503 (Invitrogen). Analyses of JFH1 were performed on a Leica SP2 confocal microscope (Leica, Heidelberg, Germany). Analysis of the Con1/C3 and the H77/C3 chimeras was performed in the same way, except that imaging was performed on a Nikon C1 confocal microscope (Nikon, Tokyo, Japan).

Electron microscopy. For conventional electron microscopy, cells cultured in plastic Petri dishes were processed *in situ*. The cells were fixed in 2.5% glutaraldehyde and 0.1 M sodium phosphate (pH 7.4), and then in OsO_4 and 0.1 M sodium phosphate (pH 7.4). The cells were then dehydrated in a graded ethanol series and embedded in an epoxy resin. Ultrathin sections were cut perpendicular to the base of the dish. For immuno-electron microscopy, cells were detached from the dish with a cell scraper after fixation in 4% paraformaldehyde, 0.1% glutaraldehyde and 0.1 M sodium phosphate (pH 7.4) for 24 h, and washed in 0.1 M lysine, 0.1 M sodium phosphate (pH 7.4) and 0.15 M sodium chloride. After dehydrating the cells in a graded series of cold ethanol, they were embedded in Lowicryl K4M at −20 °C. Ultrathin sections were labelled with primary antibodies and colloidal gold particles (15 nm) conjugated to anti-mouse IgG or anti-rabbit IgG antibodies. For double labelling, colloidal gold particles with different diameters (10 nm and 15 nm) conjugated to anti-mouse IgG or anti-rabbit antibodies were used. Samples were observed after staining with uranyl acetate and lead citrate with a JEM 1010 electron microscope at the accelerating voltage of 80 kV. Anti-Core (#32-1 and RR88), anti-NS5A (NS5ACL1) and anti-E2 (Flag M2) antibodies were used.

Preparation of the lipid droplets. Cells at a confluency of ~80% on a dish with a diameter of 14 cm were scraped in PBS. The cells were pelleted by centrifugation at 1,500 rpm. The pellet was resuspended in 500 μl of hypotonic buffer (50 mM HEPES, 1 mM EDTA and 2 mM $MgCl_2$ at pH 7.4) supplemented with protease inhibitors (Roche Diagnostics, Basel, Switzerland) and was incubated for 10 min at 4 °C. The suspension was homogenized with 30 strokes of a glass Dounce homogenizer using a tight-fitting pestle. Then, 50 μl of 10× sucrose buffer (0.2 M HEPES, 1.2 M KoAc, 40 mM $Mg(oAc)_2$ and 50 mM DTT at pH 7.4) was added to the homogenate. The nuclei were removed by centrifugation at 2,000 rpm for 10 min at 4 °C. The supernatant was collected and centrifuged at 16,000 *g* for 10 min at 4 °C. The supernatant (S16) was mixed with an equal volume of 1.04 M sucrose in isotonic buffer (50 mM HEPES, 100 mM KCl, 2 mM $MgCl_2$ and protease inhibitors). The solution was set at the bottom of 2.2-ml ultracentrifuge tube (Hitachi Koki, Tokyo, Japan). One milliliter of isotonic buffer was loaded onto the sucrose mixture. The tube was centrifuged at 100,000 *g* in an S55S rotor (Hitachi Koki) for 30 min at 4 °C. After the centrifugation, the LD fraction on the top of the gradient solution was recovered in isotonic buffer. The suspension was mixed with 1.04 M sucrose and centrifuged again at 100,000 *g*, as described above, to eliminate possible contamination with other organelles. The collected LD fraction was used for western blotting or the HCV RNA synthesis assay.

HCV RNA synthesis assay. An assay of HCV RNA synthesis using digitonin-permeabilized cells was performed as described previously[17]. For RNA synthesis assays using the LD fraction, the LD fraction collected by sucrose-gradient sedimentation was suspended in buffer B, which contained 2 mM manganese (II) chloride, 1 mg ml^{-1} acetylated BSA (Nacalai Tesque, Kyoto, Japan), 5 mM phosphocreatine (Sigma), 20 units/ml creatine phosphokinase (Sigma), 50 μg ml^{-1} actinomycin D, 500 μM ATP, 500 μM CTP, 500 μM GTP (Roche Diagnostics) and 1.85 MBq of [α-^{32}P] UTP (GE Healthcare, Little Chalfont, UK), and incubated at 27 °C for 4 h. The reaction products were analysed by gel electrophoresis followed by autoradiography.

Note: Supplementary Information is available on the Nature Cell Biology website.

ACKNOWLEDGEMENTS

We thank T. Fujimoto and Y. Ohsaki at Nagoya University for helpful discussions and technical assistance. Y.M. is a recipient of a JSPS fellowship. K.S. is supported by Grants-in-Aid for cancer research and for the second-term comprehensive 10-year strategy for cancer control from the Ministry of Health, Labour and Welfare, as well as by a Grant-in-Aid for Scientific Research on Priority Areas "Integrative Research Toward the Conquest of Cancer" from the Ministry of Education, Culture, Sports, Science and Technology of Japan. T.W. is also supported, in part, by a Grant-in-Aid for Scientific Research from the Japan Society for the Promotion of Science; and by the Research on Health Sciences Focusing on Drug Innovation from the Japan Health Sciences Foundation. R.B. is supported by the Sonderforschungsbereich 638 (Teilprojekt A5) and the Deutsche Forschungsgemeinschaft (BA1505/2-1). M.Z. and R.B. thank the Nikon Imaging Center at the University of Heidelberg for providing access to their confocal fluorescence microscopes and Ulrike Engel for the excellent support.

AUTHOR CONTRIBUTIONS

Y.M. and K.S. planned experiments and analyses. Y.M. was responsible for experiments for Figs 1, 2, 3a–c, 4a–e and 5b. K.A., N.U., electron microscopy; T.H., Fig. 1e; M.Z., R.B., Fig. S2e; and K.S. and K.W., Fig. 4f–g. T.W. provided JFH1 strain. Y.M. and K.S. wrote the manuscript. All authors discussed the results and commented on the manuscript.

COMPETING FINANCIAL INTERESTS

The authors declare no competing financial interests.

Published online at http://www.nature.com/naturecellbiology/
Reprints and permissions information is available online at http://npg.nature.com/reprintsandpermissions/

1. Martin, S. & Parton, R. G. Lipid droplets: a unified view of a dynamic organelle. *Nature Rev. Mol. Cell Biol.* **7,** 373–378 (2006).
2. Blanchette-Mackie, E. J. *et al.* Perilipin is located on the surface layer of intracellular lipid droplets in adipocytes. *J. Lipid Res.* **36,** 1211–1226 (1995).
3. Vock, R. *et al.* Design of the oxygen and substrate pathways. VI. structural basis of intracellular substrate supply to mitochondria in muscle cells. *J. Exp. Biol.* **199,** 1689–1697 (1996).
4. Liang, T. J. *et al.* Viral pathogenesis of hepatocellular carcinoma in the United States. *Hepatology* **18,** 1326–1333 (1993).
5. Moradpour, D., Englert, C., Wakita, T. & Wands, J. R. Characterization of cell lines allowing tightly regulated expression of hepatitis C virus core protein. *Virology* **222,** 51–63 (1996).
6. Deleersnyder, V. *et al.* Formation of native hepatitis C virus glycoprotein complexes. *J. Virol.* **71,** 697–704 (1997).
7. Kato, N. *et al.* Molecular cloning of the human hepatitis C virus genome from Japanese patients with non-A, non-B hepatitis. *Proc. Natl Acad. Sci. USA* **87,** 9524–9528 (1990).
8. Hijikata, M. & Shimotohno, K. [Mechanisms of hepatitis C viral polyprotein processing]. *Uirusu* **43,** 293–298 (1993).
9. Dubuisson, J., Penin, F. & Moradpour, D. Interaction of hepatitis C virus proteins with host cell membranes and lipids. *Trends Cell Biol.* **12,** 517–523 (2002).
10. Wakita, T. *et al.* Production of infectious hepatitis C virus in tissue culture from a cloned viral genome. *Nature Med.* **11,** 791–796 (2005).
11. Lindenbach, B. D. *et al.* Complete replication of hepatitis C virus in cell culture. *Science* **309,** 623–626 (2005).
12. Zhong, J. *et al.* Robust hepatitis C virus infection in vitro. *Proc. Natl Acad. Sci. USA* **102,** 9294–9299 (2005).
13. Pietschmann, T. *et al.* Construction and characterization of infectious intragenotypic and intergenotypic hepatitis C virus chimeras. *Proc. Natl Acad. Sci. USA* **103,** 7408–7413 (2006).
14. Moriya, K. *et al.* Hepatitis C virus core protein induces hepatic steatosis in transgenic mice. *J. Gen. Virol.* **78,** 1527–1531 (1997).
15. Hope, R. G., Murphy, D. J. & McLauchlan, J. The domains required to direct core proteins of hepatitis C virus and GB virus-B to lipid droplets share common features with plant oleosin proteins. *J. Biol. Chem.* **277,** 4261–4270 (2002).
16. Egger, D. *et al.* Expression of hepatitis C virus proteins induces distinct membrane alterations including a candidate viral replication complex. *J. Virol.* **76,** 5974–5984 (2002).
17. Miyanari, Y. *et al.* Hepatitis C virus non-structural proteins in the probable membranous compartment function in viral genome replication. *J. Biol. Chem.* **278,** 50301–50308 (2003).
18. Quinkert, D., Bartenschlager, R. & Lohmann, V. Quantitative analysis of the hepatitis C virus replication complex. *J. Virol.* **79,** 13594–13605 (2005).
19. Tauchi-Sato, K., Ozeki, S., Houjou, T., Taguchi, R. & Fujimoto, T. The surface of lipid droplets is a phospholipid monolayer with a unique fatty acid composition. *J. Biol. Chem.* **277,** 44507–44512 (2002).
20. Londos, C., Brasaemle, D. L., Schultz, C. J., Segrest, J. P. & Kimmel, A. R. Perilipins, ADRP, and other proteins that associate with intracellular neutral lipid droplets in animal cells. *Semin. Cell Dev. Biol.* **10,** 51–58 (1999).
21. Blight, K. J., McKeating, J. A. & Rice, C. M. Highly permissive cell lines for subgenomic and genomic hepatitis C virus RNA replication. *J. Virol.* **76,** 13001–13014 (2002).
22. Klein, K. C., Dellos, S. R. & Lingappa, J. R. Identification of residues in the hepatitis C virus core protein that are critical for capsid assembly in a cell-free system. *J. Virol.* **79,** 6814–6826 (2005).
23. Owsianka, A. *et al.* Monoclonal antibody AP33 defines a broadly neutralizing epitope on the hepatitis C virus E2 envelope glycoprotein. *J Virol* **79,** 11095–11104 (2005).
24. Ishii, N. *et al.* Diverse effects of cyclosporine on hepatitis C virus strain replication. *J. Virol.* **80,** 4510–4520 (2006).
25. Lohmann, V., Korner, F., Herian, U. & Bartenschlager, R. Biochemical properties of hepatitis C virus NS5B RNA-dependent RNA polymerase and identification of amino acid sequence motifs essential for enzymatic activity. *J Virol* **71,** 8416–8428 (1997).
26. Ohsaki, Y., Maeda, T. & Fujimoto, T. Fixation and permeabilization protocol is critical for the immunolabeling of lipid droplet proteins. *Histochem. Cell Biol.* **124,** 445–452 (2005).

nature
cell biology

Supplementary Figures and legends

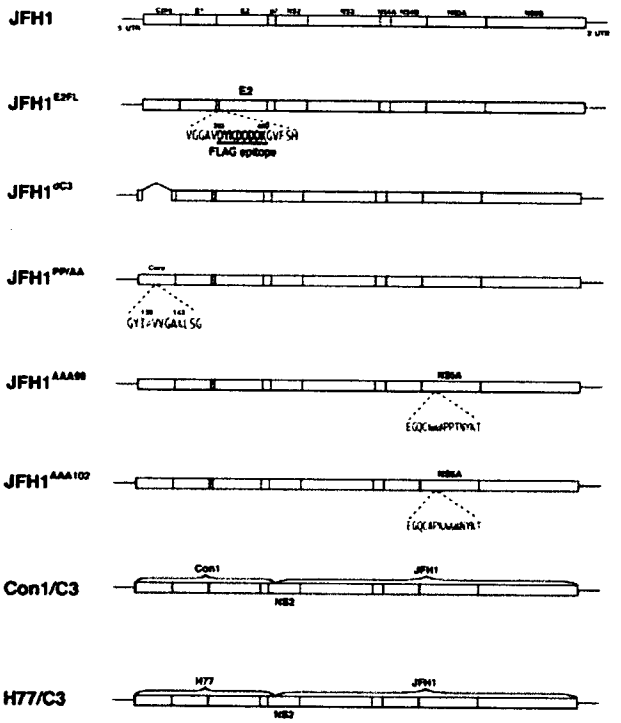

Supplementary Fig. 1

Schematic structures of HCV genomes and mutants used in this study

In JFH1^{E2FL}, the amino acid residues at positions 393 to 400 in the hyper variable region 1 of E2 were converted to a Flag epitope: DYKDDDDK. The JFH1^{E2FL} genome was used to generate other mutant variants of JFH1. In these cases the Flag epitope is marked with a blue vertical line. JFH1^{dC3} carried a deletion in the Core gene that eliminated the 17th to the 163rd amino-acid residue of Core. JFH1$^{PP/AA}$ is a mutant of JFH1^{E2FL} carrying alanine substitutions for proline residues at amino-acid positions 138 and 143 in Core. JFH1^{AAA99} and JFH1^{AAA102} contained mutated NS5A genes carrying triple-alanine substitutions for the APK sequence at amino acid positions 99 to 101 and the PPT sequence at amino acid positions 102 to 104, respectively. Constructs Con1/C3 and H77/C3 are chimeras in which the region from Core to the N-terminal domain of NS2 of JFH1 was replaced by the analogous region of the genotype 1b isolate Con1 or by the genotype 1a isolate H77[6].